PHOTOREDUCTIONS IN AQUEOUS SEMICONDUCTOR SUSPENSIONS

AND PROPERTIES OF MODIFIED POLYACRYLONITRILE FILMS

Robert Lee Calhoun, Jr. LCDR, USN

A Thesis

Submitted to

the Graduate Faculty of

Auburn University

in Partial Fulfillment of the

Requirements for the

Degree of
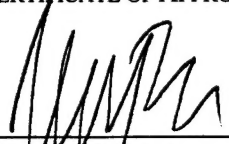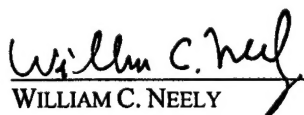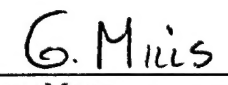
Master of Science

Auburn, Alabama

December 14, 1998

PHOTOREDUCTIONS IN AQUEOUS SEMICONDUCTOR SUSPENSIONS

AND PROPERTIES OF MODIFIED POLYACRYLONITRILE FILMS

Robert Lee Calhoun, Jr. LCDR, USN

CERTIFICATE OF APPROVAL:

JEFFREY W. FERGUS
ASSOCIATE PROFESSOR
MECHANICAL ENGINEERING

GERMAN MILLS
CHAIRMAN
ASSOCIATE PROFESSOR
CHEMISTRY

WILLIAM C. NEELY
ASSISTANT PROFESSOR
CHEMISTRY

JOHN F. PRITCHETT, DEAN
GRADUATE SCHOOL

PHOTOREDUCTIONS IN AQUEOUS SEMICONDUCTOR SUSPENSIONS

AND PROPERTIES OF MODIFIED POLYACRYLONITRILE FILMS

Robert Lee Calhoun, Jr. LCDR, USN

_____
Signature of Author

_____
Date

Copy sent to:

<u>Name</u>   <u>Date</u>

VITA

Robert Lee Calhoun, Jr., LCDR, USN, son of Robert Lee, Sr. and Gloria Ann (Flenniken) Calhoun (dec), was born December 6, 1964, in El Dorado, Arkansas. He graduated with Honors from El Dorado High School in 1983 and was appointed to the United States Naval Academy in that year. He graduated with distinction with a B.S. in Chemistry, and was commissioned an Ensign in the United States Navy in 1987. After tours as a T-34C Instructor Pilot, TRAINING SQUADRON TWO, a P-3C Patrol Plane Mission Commander, PATROL SQUADRON EIGHT, and a Catapult Officer, USS *Dwight D. Eisenhower*, CVN-69, he entered Graduate School, Auburn University, in September, 1996, under the Navy's Civilian Institutions Program. He married the former Teri Leigh Taylor of Smackover, Arkansas, on June 6, 1987, and their daughter, Margaret Caroline, was born August 19, 1993, in Brunswick, ME.

THESIS ABSTRACT

PHOTOREDUCTIONS IN AQUEOUS SEMICONDUCTOR SUSPENSIONS

AND PROPERTIES OF MODIFIED POLYACRYLONITRILE FILMS

Robert Lee Calhoun, Jr., LCDR, USN

Master of Science, December 14, 1998
(B.S., United States Naval Academy, 1987)

66 Typed Pages

Directed by German Mills

Particles of the semiconductor titanium dioxide have been shown to heterogeneously catalyze the destruction of chlorofluorocarbons (CFCs) in both air saturated and degassed aqueous suspensions. The photoreduction of CFC-11 or R-11 (CCl_3F) in this manner was studied over a range of initial R-11 concentrations, and UV light intensities. Kinetic determinations of the reduction progress were performed via ion-selective electrodes. The reduction takes place via radical chain mechanism which is eventually slowed by product poisoning of the catalyst.

Polyacrylonitrile (PAN) materials treated with methoxide ions exhibit properties typical of polymeric semiconductors. PAN-based semiconducting materials were made from textile fibers. The photochemical activity of the modified fibers was tested by attempting the photoreduction of CH_3Cl in aqueous degassed suspensions of ground fibers and sodium perchlorate. The photo-experiment was conducted similar to the experiments involving R-11 and TiO_2. Unfortunately, a byproduct of the process that forms the semiconducting fibers, OH^-, proved inseparable from the fibers and is a confirmed interference ion to determination of reaction products. Therefore, only qualitative evidence on the

phototransformation of CH_3Cl and R-11 initiated by the PAN fibers was obtained in this study. If preparation of PAN-based semiconductors is feasible, then thin films of converted PAN could lend themselves for the development of novel small scale electronic devices. In pursuit of this goal, the electrical properties of solvent cast films of solution converted PAN were studied. Preliminary results show the conductivity is in the range of high resistance semiconductors, but further improvements seemed possible by manipulations of the synthetic parameters.

ACKNOWLEDGEMENTS

TABLE OF CONTENTS

LIST OF FIGURES

INTRODUCTION

General public knowledge of semiconductors centers on crystalline silicon and its use in the electronics industry. Certainly, since the discovery of the transistor in the 1950's, electronics has been a major impact on the public at large. More recently, however, semiconductors are finding more and varied uses even in areas far away from electronic devices. Two chemicals, titanium dioxide (TiO_2), and modified polyacrylonitrile (PAN), are semiconductors and are the focus of this study.

Titanium dioxide began to receive notoriety in 1972 when it was discovered that water was split into H_2 and O_2 on the surface of TiO_2 electrodes in the presence of light.[1] At the time, this was something akin to alchemy and continued research has shown this simple, non-toxic material to be quite versatile in its role as a heterogeneous photocatalyst. More recent work has been centered on the potential use of TiO_2 for pollution cleanup in the form of wastewater treatment.[2] It seems organic molecules are susceptible to electrons and holes produced by TiO_2 when excited by light. It is in this role that TiO_2 is utilized in this work.

New advances in polymer chemistry have yielded organic molecules which may also act as semiconductors. Polyaniline is an often cited example.[3] Due to their lack of a simple crystal structure, however, the mechanism by which electricity flows through these macromolecules is poorly understood. One possibility is that long interwoven polymer chains form a band of delocalized π orbitals. These may give rise to electron mobilities that are similar to those of inorganic semiconductors with low or medium bandgap energies.

PAN, has been under investigation for some time, but not as a semiconductor. Traditionally, PAN has been used as a precursor to carbon fiber production. Various methods and degrees of heat treatment have shown PAN capable of producing very strong carbon fibers. In the early 1980's, however, groups began reporting the conductivities of PAN as it is transformed to carbon fibers.[4] A color change was noted

1

along the way and it is at this point that PAN's electrical properties improved. This work utilizes a

chemical method to affect this change, and two different aspects of semiconductor behavior are examined.

I. PHOTOREDUCTION OF TRICHLOROFLUOROMETHANE (R-11) IN AQUEOUS SUSPENSIONS OF TiO_2

Background

The tremendous release to the atmosphere and subsequent detrimental effects of chlorofluorocarbons (CFCs) have been well documented.[3] The destruction of these gases, therefore, has been of considerable interest. Industrially, high temperature/pressure catalytic hydrogenation is the preferred method because the product is the less problematic HCFC.[4] Other novel methods include thermal decomposition using reflected shockwaves[5] direct photolysis at 60°C [6], γ-radiolysis[7], various catalytic surfaces [8], and even anaerobic microbes.[9]

This work employs photoreduction using an aqueous suspension of TiO_2, a much milder and less exotic process than those listed above. First employed by Weaver et al. in the transformation of 1,1,2-trichlorotrifluoroethane (R-113), this reaction takes place at room temperature. The goal of the earlier study was to develop a TiO_2-initiated method for the phototransformation of freons using sunlight. Further objectives were that the product should be useful chemicals, in this case HCFCs, and that the process should proceed via chain reaction in order to overcome the inherent low efficiencies of semiconductor initiated photoreactions. In the present work, it was attempted to further explore this strategy by using trichlorofluoromethane (CCl_3F, R-11) as the freon to be transformed into an HCFC (dichlorofluoromethane $HCCl_2F$). The overall process is

$$CCl_3F + 2e^- \rightarrow HCCl_2F + Cl^- \quad (I-1$$

Titanium dioxide is a semiconductor which means it can produce charge carriers if hit by a photon of sufficient energy. To explain, molecular orbitals corresponding to each TiO_2 formula unit in bulk TiO_2 (consisting of a large number of formula units) are grouped together since the MOs have

3

similar energies. A group of MOs with similar energies is termed a band. Further, the group series of HOMOs is termed the valence band and the group of LUMOs the conduction band (Figure I-1). In a conductor the valence and conduction bands overlap, but in an insulator there is a difference or gap (Eg) between the bands which is large. A semiconductor, then, lies somewhere in between, usually with an Eg value corresponding to photons with $\lambda \sim 300$ - 1200 nm. Table I-1 shows the energy required to promote an electron to the conduction band for several well known semiconductors. The bandgap for the two allotropes of TiO_2 is equivalent to 375-400 nm light.

For semiconductors in contact with a solution, electrochemical models can be utilized. Conduction band electrons (e_{CB}^-) in TiO_2 would have a reduction potential of -0.5V at pH 7.[10] Note that when an electron is promoted to the conduction band, a "hole" (h_{VB}^+) is left behind in the valence band (Figure I-1). The hole also has a reduction potential, but in this case, the value is +2.7V meaning that they are powerful oxidizers. Stanbury estimated the reduction potential for R-11 to form Cl^- ions (CCl_3F/CCl_2F, Cl^-) at -0.44V[11], which means that if e_{CB}^- is involved in the reduction of R-11 via I-1, this process should proceed spontaneously with a potential of 0.06V at pH = 7.

For advantages explained later, the reaction is run at a pH of 5.9. Ward et al. have derived an expression for the potential at any pH ($E = E_0 -0.059pH$),[12] where E_0 equals -0.05 V versus SHE. This yields a potential for the reduction of R-11 by e_{CB}^- of -0.042 V at pH = 5.9, which means that the reduction process is slightly unfavorable at this pH from a thermodynamic point of view. This was also true for R-113, but to a much greater extent. These calculations have the Nernst equation as their basis and are predicated on an equilibrium situation, that is, a ratio of products and reactants. The one electron reduction of R-11 to form the halomethane radical and Cl- is irreversible since this radical decays thermally to form other products. In the absence of a stable product the Nernst equation predicts an infinite positive potential at the early stages of the reaction, meaning that this process is governed by kinetic considerations. Thus, while the system does not lend itself to equilibrium-type calculations,

conduction
band ➤

e-cb

band gap, Eg {

E

h+vb

valence
band ➤

excited state
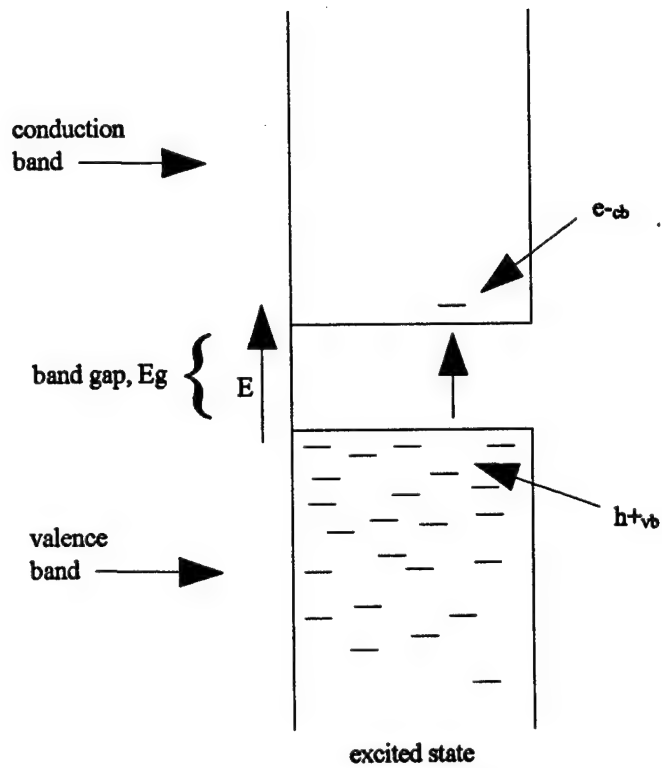
I-1 Band gap model of a semiconductor.

Table I-1 Room temperature band gaps (Eg) in eV and the corresponding wavelength for some common

semiconductors[13,14]

Substance	Band Gap (eV)	(nm)
Si	1.107	1120
GaAs	1.35	918
InP	1.27	976
ZnO	3.2	387
CdS	2.42	512
PbS	0.37	3.35 microns
GaSe	2.05	605
TiO_2 (rutile)	3.1	400
TiO_2 (anatase)	3.3	376

information obtained from these calculations gives some insight into the feasibility of a transformation via a reduction pathway.

On the other hand, freons do not undergo oxidations due to the strength of the C-Cl and C-F bonds. Furthermore, h_{VB}^+ reacts with H_2O to form ˙OH radicals when TiO_2 is in contact with H_2O. The resulting OH radicals are unreactive toward the freon.[15] However, reducing radicals can be formed when h_{VB}^+ or .OH react with molecules present in solution. These radicals may, in turn, reduce R-11 and induce chain processes, as in the case of R-113.[16]

Phototransformations of R-11 via chain reactions are very interesting since they would induce a tremendous increase in reaction efficiency. Hinshelwood cites several characteristics that various chain reactions exhibit.[17] A given reaction may not have all of them. They are as follows:

1. In photo reactions, an abnormally great quantum yield   .
2. In thermal reactions, a retardation of the change by a decrease in the dimensions of the vessel, allowing a smaller path for chains to traverse before reaching the wall
3. Acceleration of the reaction in some circumstances by the presence of an inert gas
4. An abnormal influence of the concentrations of the reacting substances on the rate
5. Reaction rates much higher than the values expected based on activation energy and collision number.
6. Sensitivity of the reaction to inhibitors
7. In certain examples, the appearance of the remarkable phenomenon of abrupt transitions from negligibly slow reaction to explosion.

Obviously, some are typical of gas phase reactions, but the concepts apply to solution phase reactions as well.[18] The slow reaction discussed in point 7 is called the induction period. As will be shown later, the photoreduction of R-11 exhibits several of the features typical of chain reactions.

There are important requirements needed in order to ensure efficient photoreactions initiated by TiO_2 particles. The first is to use a hole scavenger in order to prevent a fast charge-carrier recombination process:

$$e_{CB}^- + h_{VB}^+ \rightarrow heat \quad (I\text{-}2$$
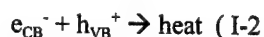
in which case the electron is lost, or trapped. Choi et al. studied various hole scavengers on a similar reaction to the one under study. Alcohols, carboxylic acids, and benzene derivatives were all used. Effects varied, but the net result was that the reaction improved when a hole scavenger was used. In the presence of an electron donor (D, or hole scavenger) the hole reacts with D through the reaction:

$$D^- + h_{VB}^+ \rightarrow {}^{\cdot}D \quad (\text{I-3}$$
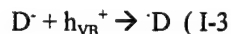
If the resulting radical (${}^{\cdot}D$) does not react fast with e_{CB}^-, then the recombination is inhibited in the presence of the electron donor. Weaver et al. used formate as their hole scavenger and studied concentration effects. They found there was an optimum concentration which yielded chain processes during the TiO_2-initiated reduction of R-113.[16]

The other important factor in TiO_2-initiated reactions is pH since the surface of the oxide particles is affected by the pH of the aqueous phase surrounding it. It must be realized that there are two fundamentally different environments available for reactions in the suspension. There is the semiconductor surface and the aqueous phase surrounding the oxide particle which is known as the "electric double layer".[19] To undergo surface reactions, a molecule must be adsorbed onto the surface. Reactions in the double layer merely require a solvated, reactive molecule to be present in the region that is close to the particle surface. When TiO_2 is placed in deionized water, the oxygen defect sites on the surface undergo the following reaction.[14]

$$O{>}Ti^+ + H_2O \rightarrow O{>}TiOH + H^+ \quad (\text{I-4}$$
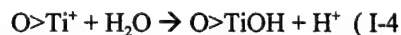
where O>Ti+ represents an oxygen deficient surface Ti atom, and O>TiOH represents the fully coordinated surface Ti atom. If the surrounding aqueous bulk is acidic, the subsequent reaction is:

$$O{>}TiOH + H^+ \rightarrow O{>}TiOH_2^+ \quad (\text{I-5}$$

and if basic:

$$O{>}TiOH + OH^- \rightarrow O{>}TiO^- + H_2O \quad (\text{I-6}$$
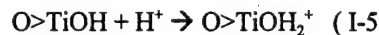
There is, of course, a pH where the competing effects are equalized and the net charge on the surface of the particle is zero. This is known as the pzc (pH at zero point charge) and is between 6.2 and 6.5 for the TiO_2 material employed in the present study. In a previous photoreduction study of R-113, it was found that, for their formate system, there was an optimum pH for the reaction as well. A formate/formic acid system buffered to pH 5.8 was utilized in that investigation. As mentioned above, this causes the particle to carry a net positive surface charge. This results in an electrostatic attraction between the oxide surface and the formate anions, which facilitates their adsorption and subsequent scavenging of the hole.

Finally, the frequency of light used to excite the TiO_2 had to be carefully selected. Transformation of halomethanes is possible by direct photolysis by light with wavelengths below 240 nm. To ensure that the observed transformation of the CFC is a semiconductor-induced reduction and not a result of direct excitation of the freon, a filter was used in order to eliminate light below 300 nm. With this arrangement, only light that can be absorbed by the semiconductor particles entered the samples.

Experimental

Sodium formate (FISCHER 99.5%), trichlorofluoromethane (ALDRICH 99%), and formic acid (FISCHER 90.8%) were used without further purification. Water used for all reactions was house distilled further purified by a Milli-Q system (MILLIPORE). The resulting resistance was 18.2 MΩ/cm. Titanium dioxide (DEGUSSA P-25) is 80% anatase and 20% rutile with a 30nm average particle size and reactive area of ~50 m^2/g. It was used as supplied by the manufacturer. Reactions were carried out in a borosilicate glass reactor with an internal volume of ~ 168mL that was manufactured by flattening one side of 1-1/2" of 2-3/4"tubing, sealing the bottom and adding two 19/38 and one 14/20 ground glass joints to the top. A 1-3/4" piece of 3-1/4" tubing was used to form a water jacket around the inner vessel. The result was a 1-1/2" x 2" double pane window through which light was directed. Suspensions were prepared by weighing out ~2.2290g of sodium formate and ~0.055g of TiO_2. One hundred mL of water and ten mL of 0.0193M formic acid were then pipetted into the reactor for a final pH of 5.88. The reactor

was then sealed with three rubber septa (SUBA); two of which were perforated and ion-selective as well as reference electrodes were introduced through the perforations, resulting in a tight seal. The mixture was stirred constantly throughout the illumination via magnetic stirbar.

Degassed reactions were purged by Ar (AIRCO) for 30 min prior to injection of the R-11. Since R-11 is aeroscopic and boils at 24°C,[20] freon was transferred from the manufacturer's bottle to a pressure tube modified with a gas tight screw-type stopcock (ACE) and equipped with a teflon/silica septa. Degassing was accomplished by three freeze-pump-thaw cycles. Transfer to the reactor was accomplished via a gas tight syringe (HAMILTON) fitted with a teflon stopcock and a #20 non-coring needle. The solubility limit of R-11 in the volume of liquid used in our experiments is 80 μL.[20] A two-phase system results: the R-11 phase consisted of droplets saturated with H_2O that migrated about the bottom of the reactor due to stirring, and on top was the aqueous TiO_2 suspension saturated with freon. Stirring of the suspensions was carried out for at least eight minutes prior to illumination to ensure saturation of the aqueous phase with the freon.

Due to the volatility of the freon, the system was under pressure and ranged from 1.4 ATM absolute for 0.1 mL of R-11 to 1.9 ATM for samples of 1.0 mL and higher. An apparatus to measure pressure was built as follows: A 15 psi gage (ASHCROFT) was fitted with 1/8" copper tubing via swedgelock®. Tygon® (5/16"OD) tubing was pushed over the copper and a male Luer-lock fitting was attached to the end. A #18 2-1/2" non-coring needle, connected via the Luer-lock, was used to pierce the septa for reading pressure at reaction termination. This was not a leak proof arrangement so any pressure changes during the reaction could not be tracked.

Illuminations were carried out by using a PTI 1010 S system with a 150W Xe arc lamp (USHIO). A GS 7-60 filter (KOPP) was used to pass 320 to 385nm light and the intensity measured by the chemical actinometer Aberchrome 540 as described by Heller.[21] Effects at ~1.8 x 10^{-5} M(hν)/min and 7.0 x 10^{-5} M(hν)/min were explored. No corrections for particle scattering were applied to reported

photonic efficiencies (ξ (Cl$^-$)). UV-Vis measurements were performed with a U-2000 spectrophotometer (HITACHI).

Reaction progress was monitored using Cl$^-$ and F$^-$ selective electrodes (ORION) and a K601 mercurous sulfate reference electrode (RADIOMETER) connected to either a PHM 85 or 95 pH meter (RADIOMETER). Calibration of the light and pH meter were done either directly prior or after a reaction. Reproducibility at high light intensities was no worse than 15%. Data at low light intensity, however, proved to vary greatly; sometimes by more than 100%. Possible causes for this behavior will be discussed later. The potentiometric determinations of halide ions were performed continuously during irradiation due to postirradiation effects. To explore possible light effects on the AgCl electrode, several blanks were run for 1 h. First, a blank utilizing formate and CFC resulted in a steady increase in potential of about 25 mV. Next, a blank was run using formate and TiO$_2$, but no CFC which resulted in a steady increase of 13 mV. Finally, a blank utilizing all constituents but no direct light showed only a 3 mV drift over an hour. However, identical results were obtained when electrode calibrations were done with TiO$_2$ and no CFC in the presence and absence of light. Thus, no appreciable light effects on the electrode were seen due to scattering by the suspension.

Gaseous products were identified by syringe extraction of 500 µL of headspace immediately after reaction termination. GC-MS measurements were made with a Finnigan 9500 GC fitted with a 5% Fluorocol column (SUPELCO), coupled to a Finnigan 3300 MS.

Results and Discussion

Photoreductions in Air-Free Systems

Shown in Figure I-2 are typical air free photoreactions for suspensions with several R-11 concentrations at a fixed light intensity (Io) of 7.0 x 10^{-5} M(hv)/min. In all cases, the change in [Cl$^-$] with time is non-linear and attempts to fit these results to a simple first order rate law were unsuccessful. Higher order rate laws were not pursued since, in our system, they lacked physical meaning. Chloride generation rates measured for R-11 were higher than those with R-113, but as in the previous
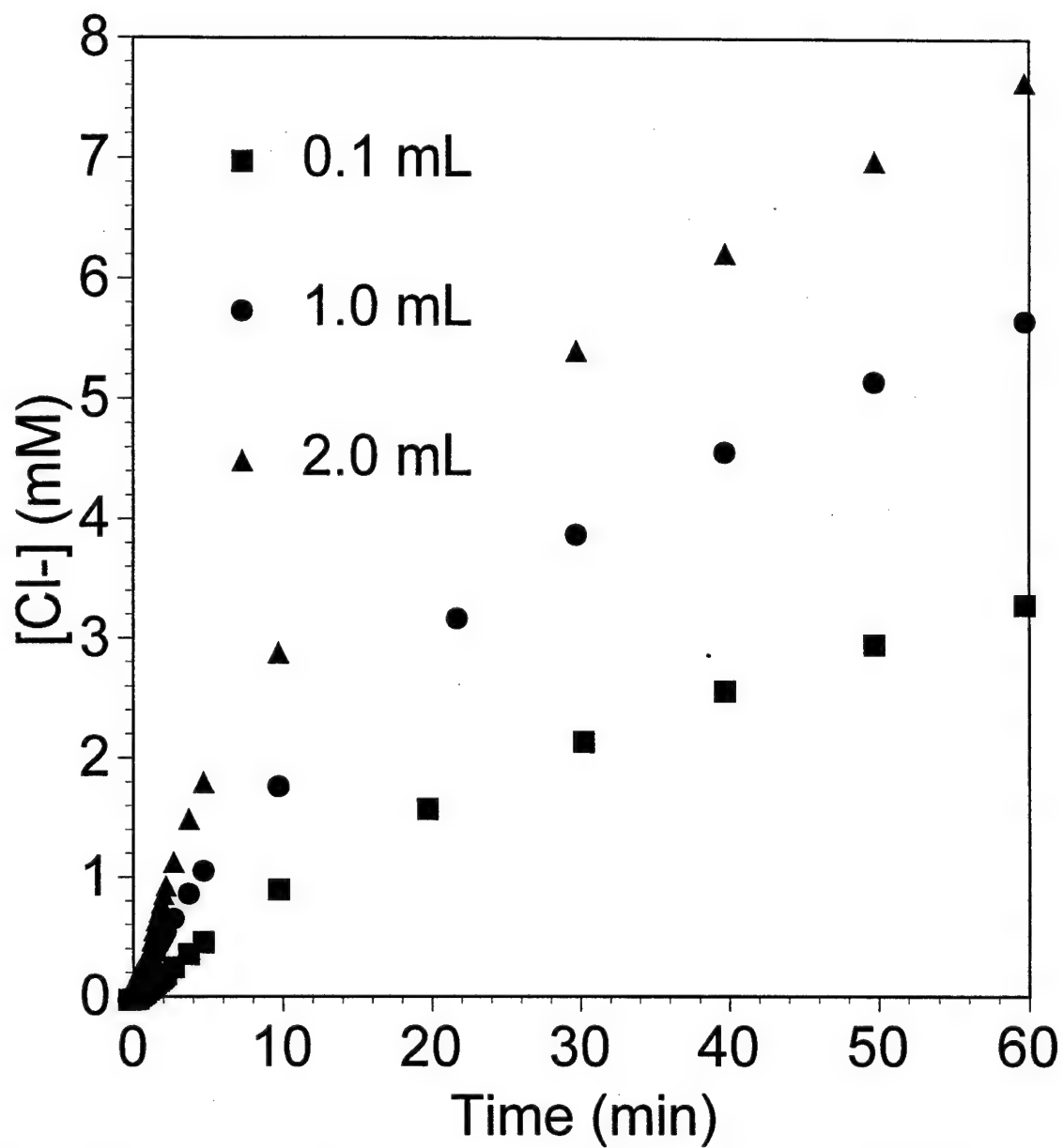
Figure I-2   Chloride production for various amounts of R-11 in 110 mL of Ar-saturated, 0.5 g/L TiO_2, 0.30 M formate/formic acid buffer, and 7.0 x 10^{-5} M(hv)/min.

investigation, an induction period was also detected, and no significant transformation of the CFC occurred in the absence of oxide particles. Figure I-3 depicts the evolution of Cl^- at short illumination times for the systems presented in Figure I-2. Only small amounts of Cl^- ions are formed during the first 2 minutes, which is referred to as the slow step, but very large increases in $[Cl^-]$ take place thereafter. Similar two-step processes occur at all R-11 concentrations. However, while the fast Cl^- ion formation step is reproducible within 15% at any particular R-11 concentration, the length of the induction period was not, and varied between 0.5 to 1.5 minutes. The induction period during the photoreduction of R-113 was explained by assuming that traces of O_2 were present in the system, which reacts with the reducing species generated by illumination of TiO_2 particles in the presence of HCO_2^-:

$$TiO_2 + h\nu \rightarrow e_{CB}^- + h_{VB}^+ \quad (\text{ I-7}$$

$$h_{VB}^+ + H_2O \rightarrow {}^{\cdot}OH + H^+ \quad (\text{ I-8}$$

$$h_{VB}^+ + HCO_2^- \rightarrow {}^{\cdot}CO_2^- + H^+ \quad (\text{ I-9}$$

$${}^{\cdot}OH + HCO_2^- \rightarrow {}^{\cdot}CO_2^- + H_2O \quad (\text{ I-10}$$

$$e_{CB}^- + O_2 \rightarrow {}^{\cdot}O_2^- \quad (\text{ I-11}$$

$${}^{\cdot}CO_2^- + O_2 \rightarrow {}^{\cdot}O_2^- \quad (\text{ I-12}$$
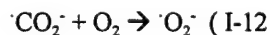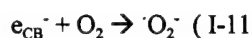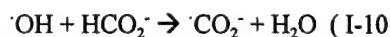
Evidence for step I-8 was obtained during investigations of the "current doubling" effect seen in HCO_2^- solutions with TiO_2.[22] A similar process is expected to take place in suspensions containing R-11. Because ${}^{\cdot}O_2^-$ does not initiate reduction of the freon, but is ultimately reduced to form H_2O, it competes with CCl_3F for reductive agents such as e_{CB}^- and ${}^{\cdot}CO_2^-$ formed through steps.

The induction period ceases once most of the O_2 molecules are removed from the system through their reduction to water, at which point the fast reduction of CCl_3F starts. The induction period is short in degassed samples because the amount of air present in these systems is very small, resulting most probably from leaks incurred during the transfer of R-11 from the degassing reservoir to the photoreactor or the few ppm O_2 present in the Ar.
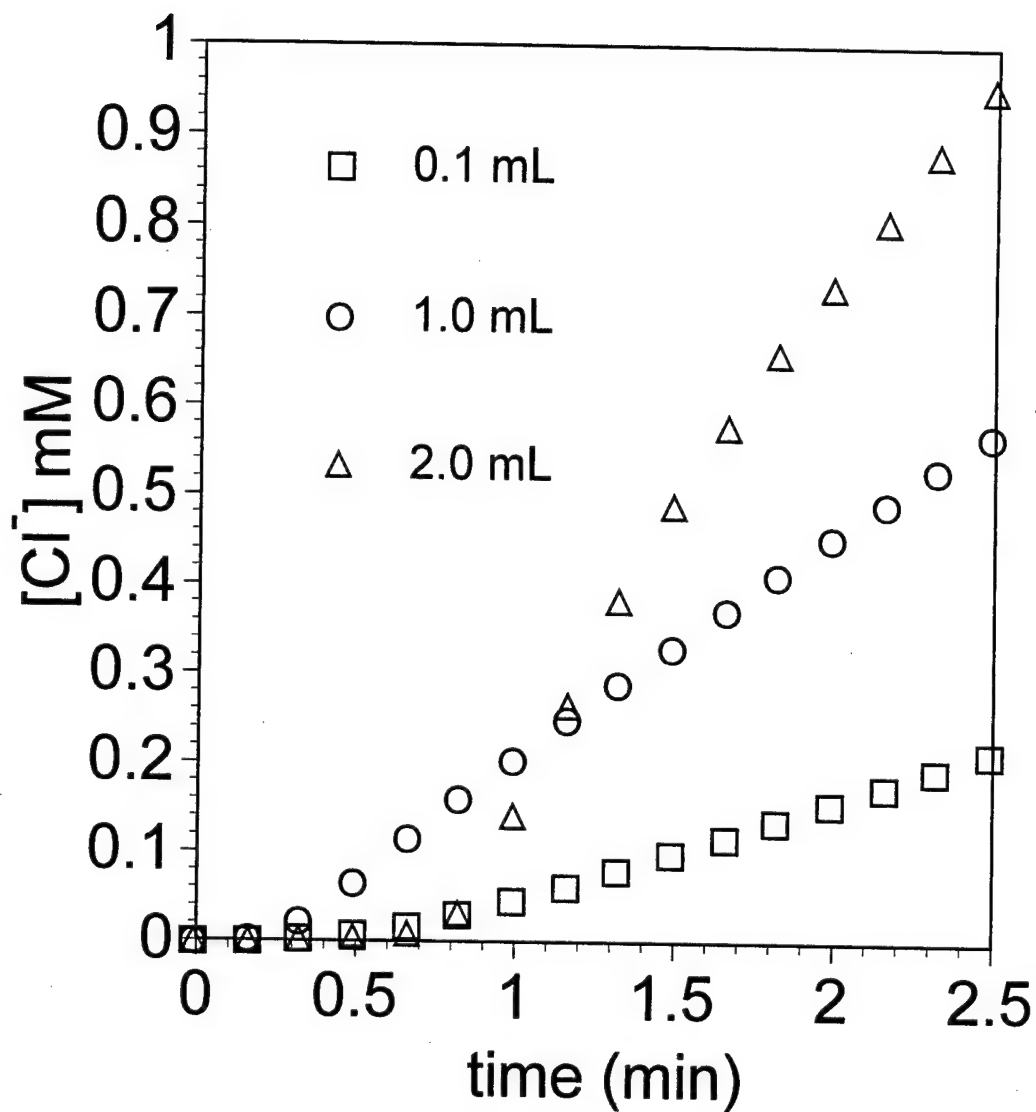
Figure I-3   Chloride production at short times for various amounts of R-11 in 110 mL of Ar-saturated, 0.5 g/L TiO_2, 0.30 M formate/formic acid buffer, and 7.0 x 10^{-5} M(hv)/min.

In contrast to the slow increases of [Cl⁻] at short illumination times, large amounts of Cl⁻ ions are formed during the fast step. Since [Cl⁻] evolves in a non-linear fashion with time, initial rates of Cl⁻ ion generation (R) were calculated from the near linear increase of Cl⁻ during the early stage of the fast step shown in Figure I-3 in order to compare reaction rates gathered under variable experimental conditions. These rates were then converted to photonic efficiencies,

$$\xi\,(Cl^-) = R/I_o$$

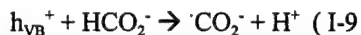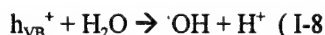where $R = d[Cl^-]/dt$ = initial rate of Cl⁻ generation. Photonic efficiencies refer to the number of moles of product generated per mole of photons of light entering the photoreactor and are not corrected for losses of photons due to scattering. The $\xi\,(Cl^-)$ values represent lower limits of quantum yields and, in our systems, photonic efficiencies higher than one indicate the occurrence of chain processes.

Figure I-4 shows the values of $\xi\,(Cl^-)$ as a function of the amount of R-11 introduced into the suspensions. For all amounts of R-11 used (0.1 mL to 4.0 mL), the solubility in water of the freon was exceeded. This is evidenced by post reaction pressure measurements, which show significant readings above one atmosphere. Since the pressure inside the vessel is atmospheric after degassing the suspensions with Ar, any pressure increase would be due to the introduction of the freon and/or the formation of gaseous products. While the latter is true, evaluation of Figure I-2 shows the reaction proceeds with about 10% yield which could not account for such a significant increase in internal pressure. Also of note is that the increase in pressure does not increase the solubility significantly. Post-reaction pressure for 0.1 mL of R-11 is 1.4 ATM which shows a significant amount of R-11 in the gas phase, but this quantity of the freon is only 20 µL more than the solubility limit of freon in 110 mL of water. Yet, as Figure I-4 shows, increasing amounts of CFC yield faster and faster reactions. Since continuous stirring induced formation of small freon droplets, it seems that freon molecules from the droplets can contribute to the propagation of the chain process. Thus, having R-11 dissolved in the aqueous phase does not ensure efficient chain processes, which occur mainly if freon molecules are located close to the oxide particles.

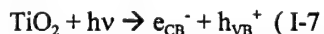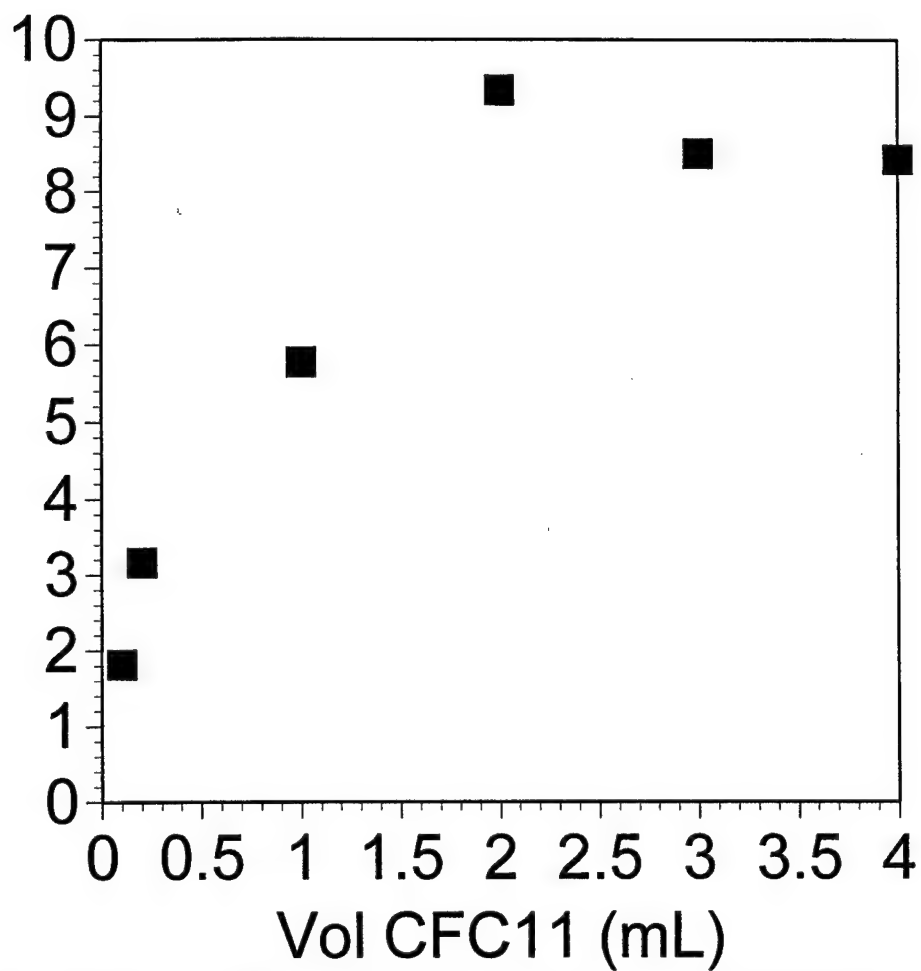Figure I-4 Photonic efficiencies for the fast step of various amounts of R-11 in 110 mL of Ar-saturated, 0.5 g/L TiO_2, 0.30 M formate/formic acid buffer, and 7.0 x 10^{-5} M(hν)/min

These results indicate that the dechlorination of R-11 proceeds through a chain reaction. An alternative process, where the illuminated particles induce complete dechlorination of the freon molecules via a thermal reaction following an initial one-electron reduction step of the CFC by e_{CB}^- and/or $\cdot CO_2^-$, followed by:

$$\cdot CCl_2F \rightarrow 2Cl^- + F^- + products \quad (\text{I-13}$$
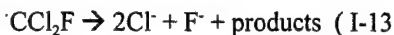
which predicts a maximum value of ξ (Cl^-) $\leq$ 3, and a ratio of concentrations of $[Cl^-]/[F^-]$ = 3 for all reaction times.

Evidence for the formation of F^- ions is presented in Figure I-5; these data correspond to the simultaneous formation of Cl^- and F^- in an illuminated, degassed suspension containing 2ml of R-11. During the induction period, the concentration ratio $[Cl^-]/3[F^-] \sim 1$, but at longer times the ratio is much higher than one and increases with time. This is an indication that chloride ions are formed more efficiently than fluoride ions, the latter being formed most probably through a side reaction. Thus, this mechanism represented by steps I-13 and I-14 (see below) is inconsistent with the results of Figure I-5. Furthermore, the data of Figure I-4 indicates that ξ (Cl^-) = 1.8 for 0.1mL of freon and increases with increasing amounts of freon to reach values of about ξ (Cl^-) = 9 at CFC volumes of 2mL and higher.

As in the case of the chain photoreduction of R-113, an HCFC is the expected product of the TiO_2 initiated transformation of R-11. Results from GC/MS analysis of the head space gas from a suspension with 0.5g/L TiO_2, 2mL freon, 0.3M formate/formic acid buffer, and illuminated for one hour are in line with expectations.

According to the MS spectrum, the gas sample contains Ar, traces of air, CO_2, the starting material-R-11, CCl_2F_2 (R-12, which is present as an impurity in the commercial samples of R-11) and $HCCl_2F$. The latter HCFC is the expected product from a reductive chain process involving $\cdot CO_2^-$ radicals as chain carriers. Therefore, the kinetic results of Figure I-4 in conjunction with the GC/MS data are consistent with a chain mechanism analogous to that of the transformation of R-113. This mechanism
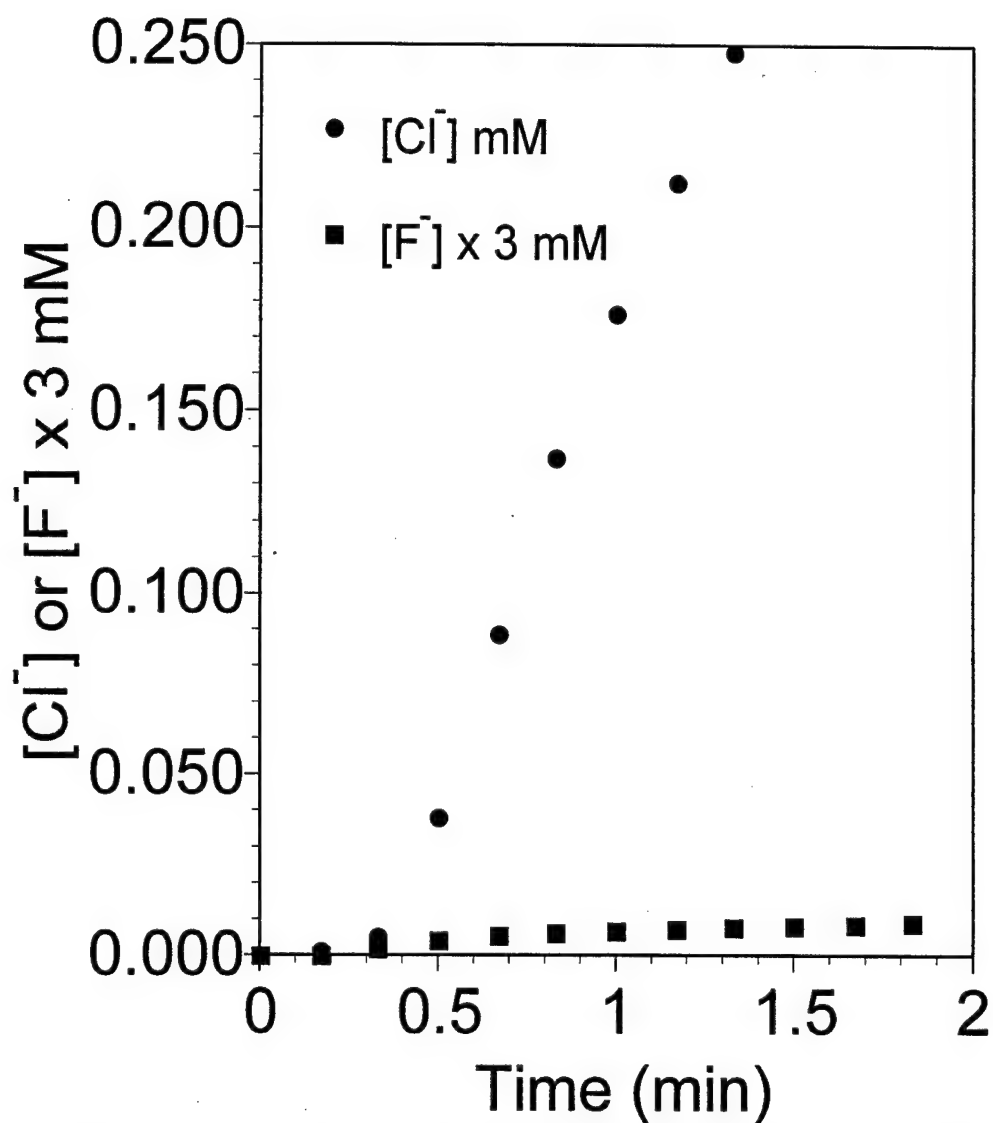
Figure I-5 Chloride and fluoride production of 2 mL of R-1111 in 110 mL of Ar-saturated, 0.5 g/L TiO_2, 0.30 M formate/formic acid buffer, and 7.0 x 10^{-5} M(hv)/min.

consists of elementary steps I-7 through I-10 followed by:

$$e_{CB}^- + CCl_3F \rightarrow Cl^- + \cdot CCl_2F \quad (\text{I-14}$$

$$\cdot CO_2^- + CCl_3F \rightarrow Cl^- + CO_2 + \cdot CCl_2F \quad (\text{I-15}$$

$$\cdot CCl_2F + HCO_2^- \rightarrow HCCl_2F + \cdot CO_2^- \quad (\text{I-16}$$
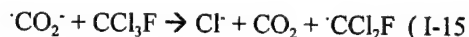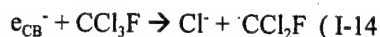
Our experimental observations are explained under the assumption that termination occurs

through reduction of the freon radical to form a carbene as was observed in the TiO_2 induced

photoreduction of CCl_4.[23]

$$\cdot CCl_2F + \cdot CO_2^- \rightarrow :CClF + Cl^- + CO_2 \quad (\text{I-17}$$

$$:CClF + H_2O \rightarrow CO + 2H^+ + Cl^- + F^- \quad (\text{I-18}$$
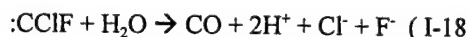
Step I-18 predicts the formation of CO as a reaction product, and a signal corresponding to this

compound ($m/e = 28$) is detected during GC/MS analysis. However, confirmation of the formation of CO

requires further work since the peak with $m/e = 28$ may also result from small amounts of N_2 that

inevitably leak into the syringes containing the headspace samples during their transfer to the GC/MS

instrument. The experimental data does not support alternative termination steps based on dimerization

reactions of chain carriers:

$$\cdot R + \cdot R \rightarrow R\text{-}R \quad (\text{I-19}$$

where $R = \cdot CCl_2F$ or $\cdot CO_2^-$. Termination via dimerization of $\cdot CCl_2F$ radicals is not consistent

with the GC/MS data since the product of such a reaction ($FCl_2C\text{-}CCl_2F$, 1,1,2,2-

tetrachlorodifluoroethane) was not detected. A termination step through dimerization of $\cdot CO_2^-$ radicals to

yield oxalate is also possible but such a reaction fails to account for the F^- ions that are formed as side

products (see Figure I-5).

The chain photoreduction of R-11 in air-free systems to form $HCCl_2F$ proceeds according to the

overall reaction I-1 is represented by steps I-7 through I-10 and I-14 to I-18. According to this

mechanism, not only e_{CB}^- but also $h_{VB}+$ contribute to the reduction of the CFC because the oxidizing hole is converted into the strongly reducing $^{\cdot}CO_2^-$ radical ($E^0 = -1.8V$ for $CO_2/\ ^{\cdot}CO_2^-$).[24]

Although the photonic efficiency for the formation of charge carriers in I-7 is $\xi = 1$ (by definition), the photonic efficiency of reducing species that react with R-11 (e_{CB}^- and $^{\cdot}CO_2^-$) is much less than one. This is a consequence of fast recombination of charge carriers within the semiconductor particles.[25] It has been estimated that about 60% of the photogenerated electrons are lost even in the presence of an efficient hole scavenger such as n-propanol.[26] Therefore, an important question is the photonic efficiency of reducing agents that initiate the reduction of R-11 in our systems containing HCO_2^- as electron donor. An estimate of ξ (e_{CB}^-) and ξ ($^{\cdot}CO_2^-$) in formate containing TiO_2 suspensions was obtained in previous investigations using methylviologen (MV^{+2}).[27] This redox indicator has a reduction potential very similar to that of R-11 ($E^0 = -0.44V$ for $MV^{+2}/MV^{+\cdot}$, where $MV^{+\cdot}$ is the reduced form of MV^{+2}). MV^{+2} is reduced according to:

$$MV^{+2} + e_{CB}^- \rightarrow MV^{+\cdot} \quad (\text{I-20}$$

$$MV^{+2} + {}^{\cdot}CO_2^- \rightarrow MV^{+\cdot} + CO_2 \quad (\text{I-21}$$
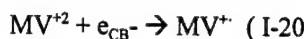
Using a light intensity similar to the one employed in the present investigation ($Io = 4.1 \times 10^{-5}$ M(hν)/min) it was found that ξ (MV^+) = 0.19, this value corresponding to the combined quantum efficiencies of e_{CB}^- and $^{\cdot}CO_2^-$ that are available to react with R-11. From the results of Figure I-4 it follows that the maximum kinetic chain length is about 50 for suspensions with volumes of CFC ≥ 2 mL. Hence, on average every reducing species that is photogenerated induces transformation of about 50 CCl_3F molecules to $HCCl_2F$.

Air-saturated Systems

Among the characteristics of chain reactions cited by Hinshelwood is their sensitivity to inhibitors. Considering that the process investigated in our study is a reduction reaction, and that O_2 is a well known inhibitor of free radical reductions, it seems logical to expect a strong inhibition of the R-11

photoreduction induced by oxygen. In fact, the induction periods shown in Figure I-3 for degassed samples were explained earlier on the basis of an inhibiting effect induced by traces of oxygen present in those samples. Much stronger inhibitions were expected in suspensions saturated with air due to the much higher concentration of oxygen molecules present in these samples.

Presented in Figure I-6 is the evolution of [Cl⁻] vs. time for an air-saturated suspension containing several volumes of R-11, 0.5g/L TiO_2, and 0.3M of the formate/formic acid buffer. In these systems, as well as in all suspensions saturated with air, the induction period is very long (between 25 and 35 minutes) as compared with that of a similar system that is Ar-saturated (Figure I-3). Figure I-7 shows the changes of [Cl⁻] and [F⁻] generated during the induction period for a suspension with 2 mL of R-11 sample. It is clear that during this period [Cl⁻]/[F⁻] ~ 3, but after the induction period is over, [Cl⁻] >> [F⁻]. These results mean that during the period where O_2 interferes with the chain reduction of the CFC a different process takes place leading to the complete dehalogenation of the freon. In other words, at high [O_2], this compound not only inhibits the freon reduction via steps I-11 and I-12, it also changes the mechanism by which R-11 is transformed, leading to a different product distribution. The following mechanism accounts for the CFC transformation during the induction period in air-saturated suspensions:

$$\cdot CCl_2F + O_2 \rightarrow \cdot O_2CCl_2F \quad (\text{I-22}$$

$$\cdot O_2^- + H^+ + \cdot O_2CCl_2F \rightarrow O_2 + HO_2CCl_2F \quad (\text{I-23}$$

$$e_{CB}^-/.CO_2^- + H+ + \cdot O_2CCl2F \rightarrow HO_2CCl_2F /+ CO_2 \quad (\text{I-24}$$

$$2HO_2CCl_2F \rightarrow O_2 + 2HOCCl_2F \quad (\text{I-25}$$

$$HOCCl_2F \rightarrow OCClF + H^+ + Cl^- \quad (\text{I-26}$$

$$\cdot OCClF + H_2O \rightarrow CO_2 + Cl^- + F^- + 2H^+ (\text{I-27}$$
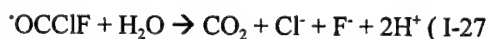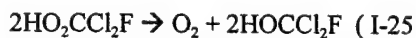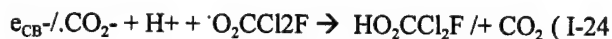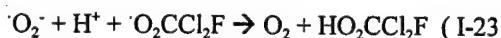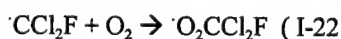
Figure I-6   Chloride production for various amounts of R-11 in 110 mL of air-saturated, 0.5 g/L TiO$_2$, 0.30 M formate/formic acid buffer, and 7.0 x 10^{-5} M(hν)/min.

Figure I-7 Chloride and fluoride production of 2 mL of R-1111 in 110 mL of air-saturated, 0.5 g/L TiO_2, 0.30 M formate/formic acid buffer, and 7.0 x 10^{-5} M(hv)/min.
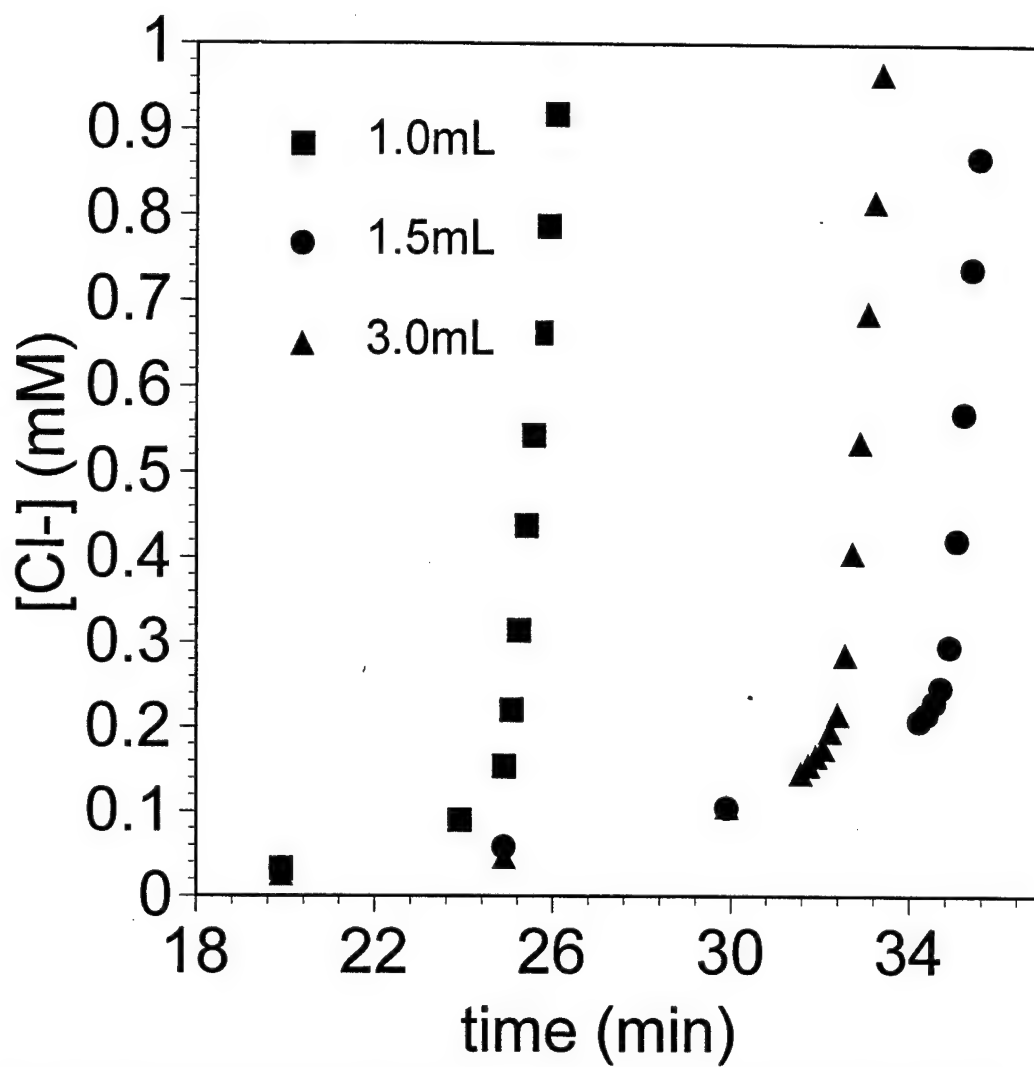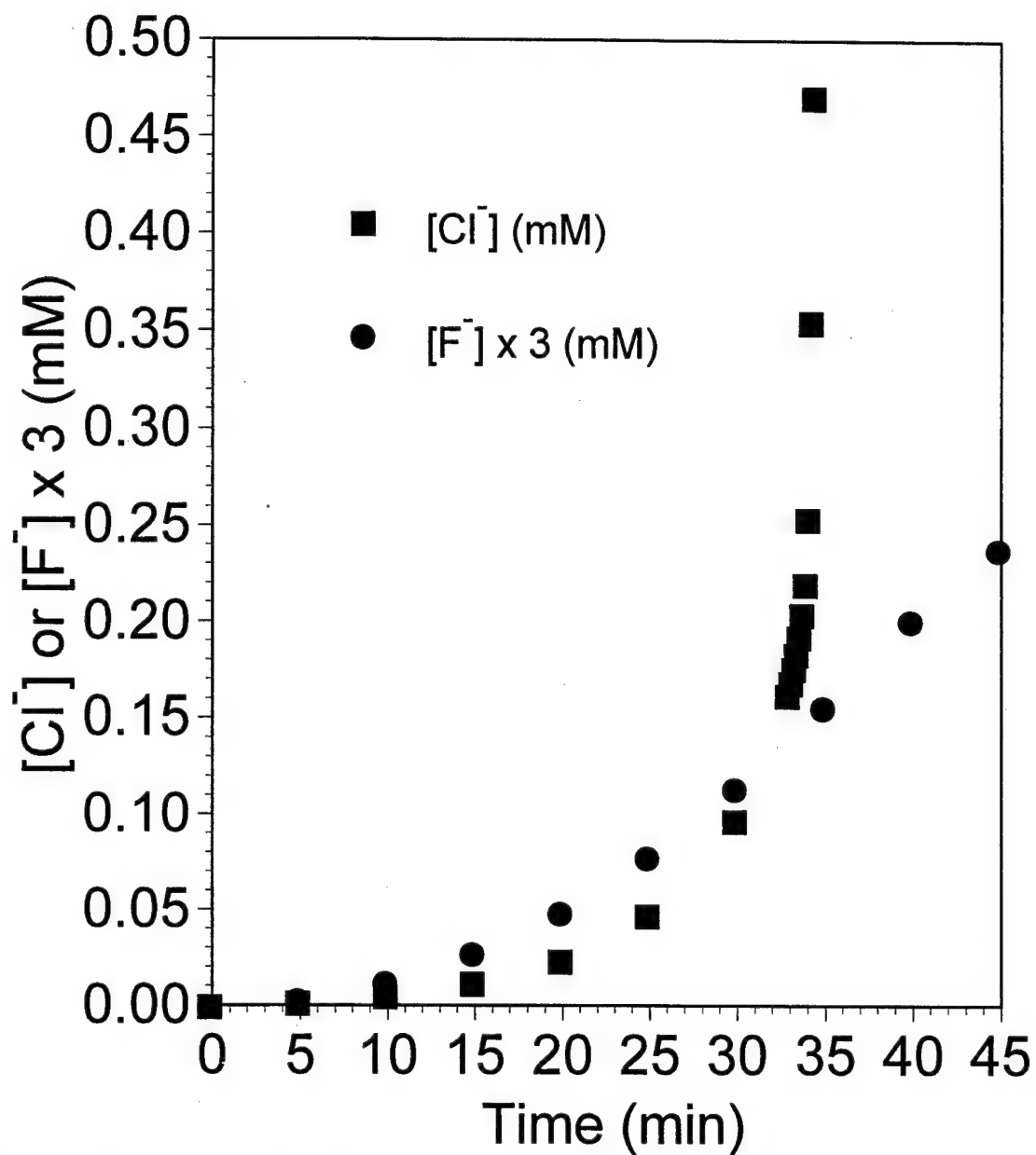
This mechanism is similar to the one proposed for the reductive dechlorination of CCl_4, which leads to the generation of 4 Cl^- ions and CO_2 in air containing systems.[23] Interestingly, 4 oxygen molecules participate in the process described by steps I-22 to I-27 However, only one O_2 molecule is irreversibly reduced in this process. This implies that elimination of O_2 is slow in these systems, leading to long induction periods. Although the induction periods of both Ar-saturated and in air saturated suspensions can be related in a qualitative fashion to the presence of O_2, different processes take place in each system due to their different $[O_2]$. In degassed suspensions, R-11 competes with the few O_2 molecules present for the reducing species (e_{CB}^- and CO_2^-), but it is expected that most of the reducing species are scavenged by the freon due to the much higher CFC concentration in these systems. Consequently, a significant amount of CCl_2F radicals are formed via steps I-14 and I-15, and the decay of the freon radicals proceeds during the induction period through both the chain reaction, and the oxidation mechanism represented by steps I-22 through I-27. The fact that both chain and freon oxidation processes occur in parallel explains the ξ (Cl^-) values measured during the slow step that range from 8 x 10^{-2} to 0.23. Reproducibility of these photonic efficiencies is poor due to limitations in data collection imposed by the sensitivity of the Cl^- electrode and by the brevity of the induction period in Ar-saturated suspensions. However, these values of ξ (Cl^-) are at least 7 times larger than the corresponding ξ (Cl^-) results of air saturated suspensions presented in Figure I-8. In air-containing suspensions, O_2 can compete successfully with R-11 for the photogenerated reducing species, yielding O_2^- (not CCl_2F) as the main product of the consumption of e_{CB}^- and CO_2^-. Because this radical is unable to reduce R-11, only the few freon molecules that can scavenge photogenerated reducing species undergo transformation. Furthermore, all formed CCl_2F radicals react then with O_2 via step I-22, meaning that no chain transformation of R-11 are possible during the induction period in these systems.

Steep increases of [Cl-] are detected in air-saturated samples once the induction period is over, see Figure I-6. Depicted in Figure I-9 are ξ (Cl^-) values vs. volume of added freon calculated from the fast increases in [Cl^-]. Photonic efficiencies increased continuously with raising volume of CFC from

Figure I-8 Photonic efficiencies for the fast step of various amounts of R-11 in 110 mL of air-saturated, 0.5 g/L TiO_2, 0.30 M formate/formic acid buffer, and 7.0 x 10^{-5} M/min

4.2 at 0.1 mL R-11 to 15 for a CFC volume of 1.5 mL, and remained constant thereafter. Surprisingly, these photonic efficiencies are 50-100% higher than the corresponding values of Ar-saturated systems shown in Figure I-4. As will be shown later, the chain reduction of R-11 is suppressed by the presence of Cl⁻ ions. Accordingly, more efficient reduction of the CFC is expected to take place in systems where very low [Cl⁻] are generated during the induction period prior to the fast step. Table I-2 compares the chloride ion concentrations present at the time when the fast Cl- generation starts for air and Ar-saturated suspensions with different volumes of CFC. Ar-saturated suspensions have less Cl- present before the fast step occurs, indicating that the lower ξ (Cl⁻) values of these systems are not explained by Cl⁻ induced inhibitions of the chain transformation.

From the data of Figure I-7, it is clear that no chain reaction takes place during the induction period in air saturated suspensions since [Cl⁻]/[F⁻] ~ 3. Ratios of [Cl⁻]/[F⁻] much higher than 3 are observed after the induction period in Figure I-7. This implies that most of the O_2 present in the samples is reduced during the induction period, and that the fast Cl⁻ formation step occurring at longer times is related to the chain reduction process of R-11 in Ar-saturated systems. However, the chain process represented by steps I-14 through I-18 alone cannot account for the fast step in samples that initially contained air, otherwise identical values of ξ (Cl⁻) for the fast step are to be expected in Ar or air-saturated suspensions. The higher ξ (Cl⁻) values shown in Figure I-9 suggest that an additional process takes place at longer times in these systems. Assuming the steady state [O_2] during the first process is much lower than steady state oxygen concentration during the induction period, it is possible, in principle, to reach conditions under which reduction of ˙O_2CCl_2F radicals (step I-23) is no longer efficient since formation of ˙O_2^- via step I-11 or I-12 is no longer viable. Peroxy radicals such as ˙O_2-R are known to persist for long times but decay via:

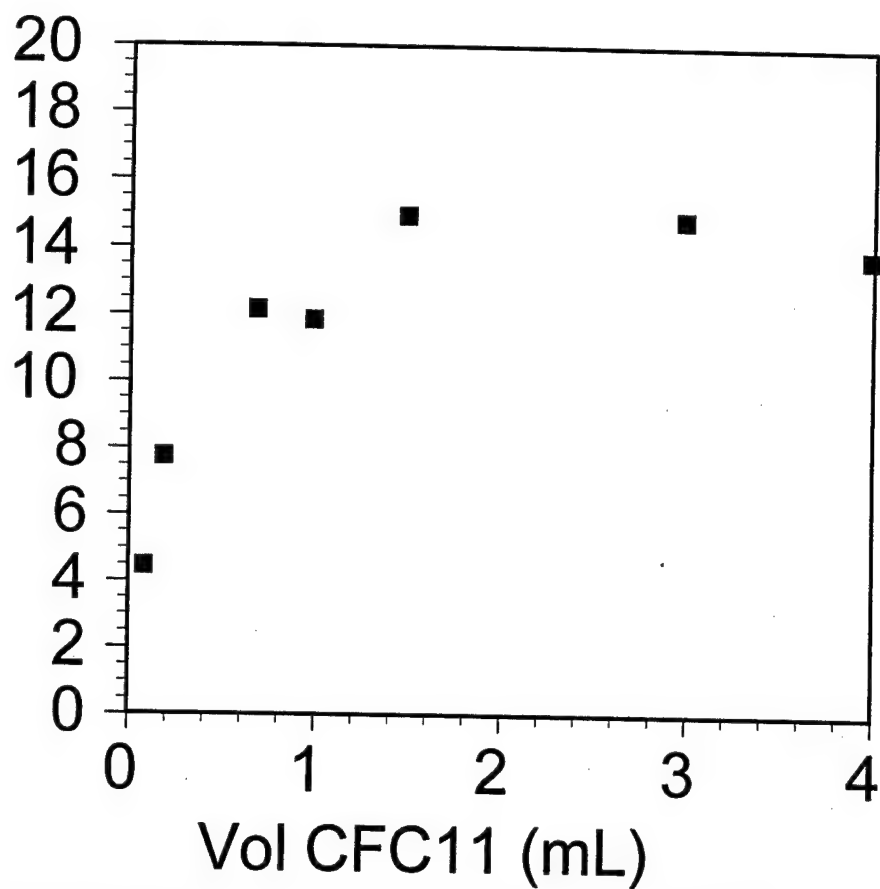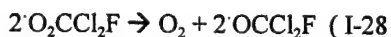$$2˙O_2CCl_2F \rightarrow O_2 + 2˙OCCl_2F \quad (\text{I-28}$$

Figure I-9 Photonic efficiencies for the slow step of various amounts of R-11 in 110 mL of air-saturated, 0.5 g/L TiO_2, 0.30 M formate/formic acid buffer, and 7.0 x 10^{-5} M/min

Table I-2

Volume R-11 (mL)	0.1	0.2	1.0	1.5	2.0	3.0	4.0
[Cl-] (mM) in Argon[a]	0.018		0.022		0.032	0.011	0.02
[Cl-] (mM) in air[a]	0.15	0.14	0.14	0.23		0.32	0.36

a: [Cl-] in mM at the beginning of the fast step in both air and Ar-saturated solutions of R-11 in

110 mL of 0.5g/L TiO_2, 0.30M formate/formic acid, and 7.4×10^{-5} M(hv)/min.

The resulting oxygen-centered radical is a strong oxidizer which is expected to abstract H-atoms from HCO_2^-:

$$\cdot OCCl_2F + HCO_2^- \rightarrow HOCCl_2F + \cdot CO_2^- \quad (\text{I-29}$$

Formation of another $\cdot CO_2^-$ radical through the last step implies that chain transformations may be initiated again. In other words, the chain transformation of R-11 is no longer terminated by O_2 under these conditions. Furthermore, both chain reduction and oxidative decay of some of the $\cdot CCl_2F$ radicals may now take place simultaneously, leading to higher Cl^- rates of formation as compared with those of Ar-saturated suspensions.

Light Intensity Effects

Light-initiated free radical chain reactions are very sensitive to the intensity of the incident photon flux. Recent studies on polymerizations and transformations of freons have demonstrated that this is also the case for chain processes initiated by semiconductor particles.[2,3] In general, photonic efficiencies decrease with increasing I_o because the steady-state concentrations of chain carriers increase at higher light intensities, which accelerates radical-radical termination steps such as I-17 and I-19.

Figure I-10 is a plot of ξ (Cl^-) for various volumes of R-11 in Ar-saturated suspensions using $I_o = 1.8 \times 10^{-5}$ M(hv)/min. It should be noted that these experiments were performed under conditions identical to those of Figure I-4, except that I_o was about 4 times lower in the experiments presented in Figure I-10. Comparison of the two sets of data indicates that, in general, photonic efficiencies are between 2.5 to 5 times higher at the lower I_o. However, the ξ (Cl-) values fluctuate significantly at the lower light intensity, with deviations as large as 100% in some cases. This lack of reproducibility was also noticed in the previous study of R-113, although the irreproducibility problem was detected only at $I_o < 4 \times 10^{-6}$ M(hv)/min.[16] Since this problem is not significant in the present system at the higher light intensity used in most of our experiments ($I_o \geq 6.5 \times 10^{-5}$ M(hv)/min.), it is reasonable to assume that the irreproducibility problem may be related to small leaks of air into the samples.
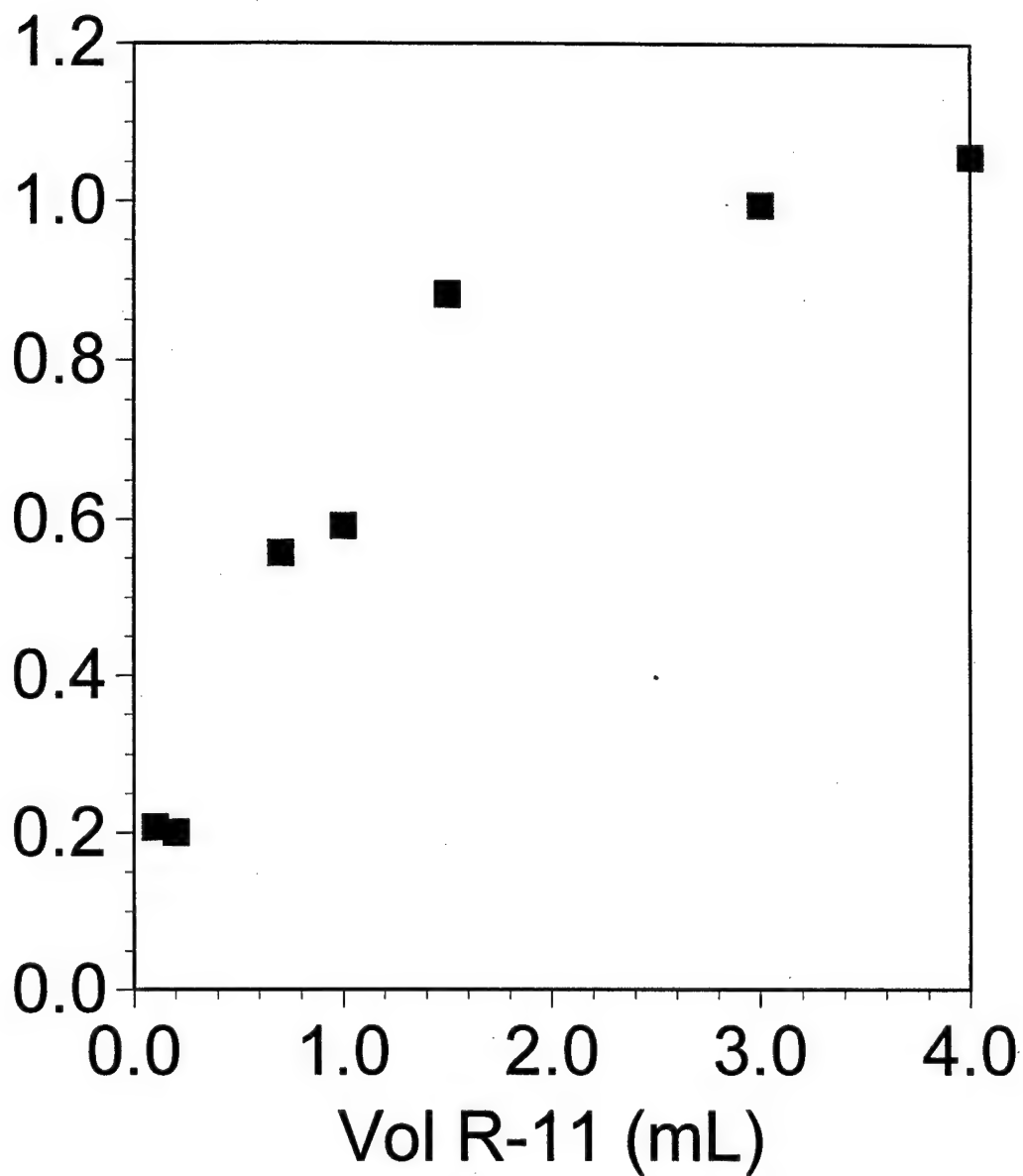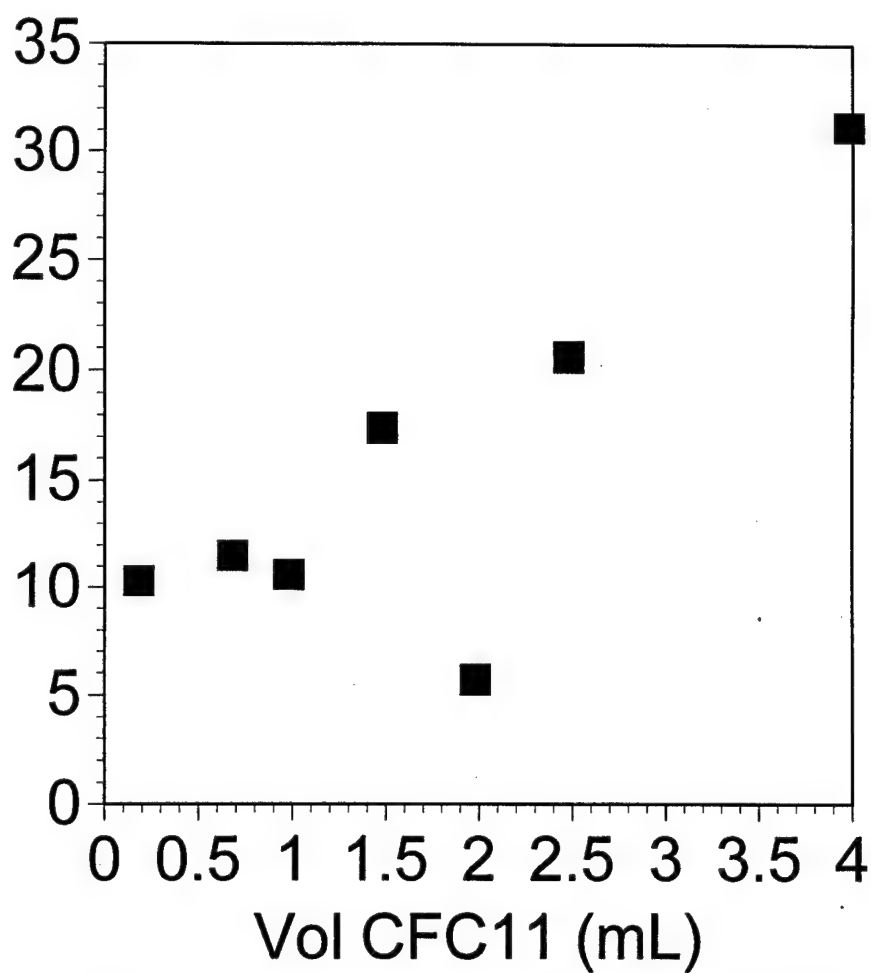
Figure I-10 Photonic efficiencies for the fast step of various amounts of R-11 in 110 mL of air-saturated, 0.5 g/L TiO_2, 0.30 M formate/formic acid buffer, and 1.8 x 10^{-5} M/min

Higher concentrations of reducing radicals form at high Io, and the reduction of any traces of O_2 is faster than in illuminations with low light intensities, where only small concentrations of e_{CB}^- and $\cdot CO_2^-$ are formed.

An alternatively possibility is that a long living inhibitor may form during the induction period. Possible inhibitors are H_2O_2 or HO_2CCl_2F which may aid chain termination via hydrogen atom abstractions by the CFC radical:

$$\cdot CCl_2F + HO_2\text{-}R \rightarrow HCCl_2F + \cdot O_2\text{-}R \quad (\text{I-30}$$

(where R = H or $\cdot CCl_2F$), followed by reduction of $\cdot O_2$-R via steps I-23 or I-24. Since HO_2-R decays faster through step I-25 with increasing peroxide concentrations, that is, at higher light intensities, step I-30 is significant only at low Io where the organic peroxide survives for longer times.

Post-irradiation Effects

Post irradiation formation of products is frequently observed in chain reactions, and two different experiments were performed to test for such processes in our system. The first experiment consisted of illuminations for 3 minutes alternating with periods of no direct illumination of similar length (curve 1). In the second experiment (curve 2), [Cl$^-$] changes were measured continuously after the initial irradiation period of 3 min. Since chloride ions continued to form during the first 30 minutes, the sample was illuminated again (for 3 minutes) at that time. A smaller post irradiation Cl$^-$ formation became very slow after a few minutes. Hence, subsequent irradiation periods of 3 minutes were performed once the preceding post irradiation reaction slowed down significantly. Results from the experiments are presented in Figure I-11; strong post irradiation effects are evident from both curves.

Larger increases of [Cl$^-$] are noticed during the illumination periods in both sets of data. This is particularly evident in curve 2 since a much steeper change in Cl$^-$ concentration occurs when the suspension left to react thermally for 27 minutes is illuminated again. Although the subsequent speeds
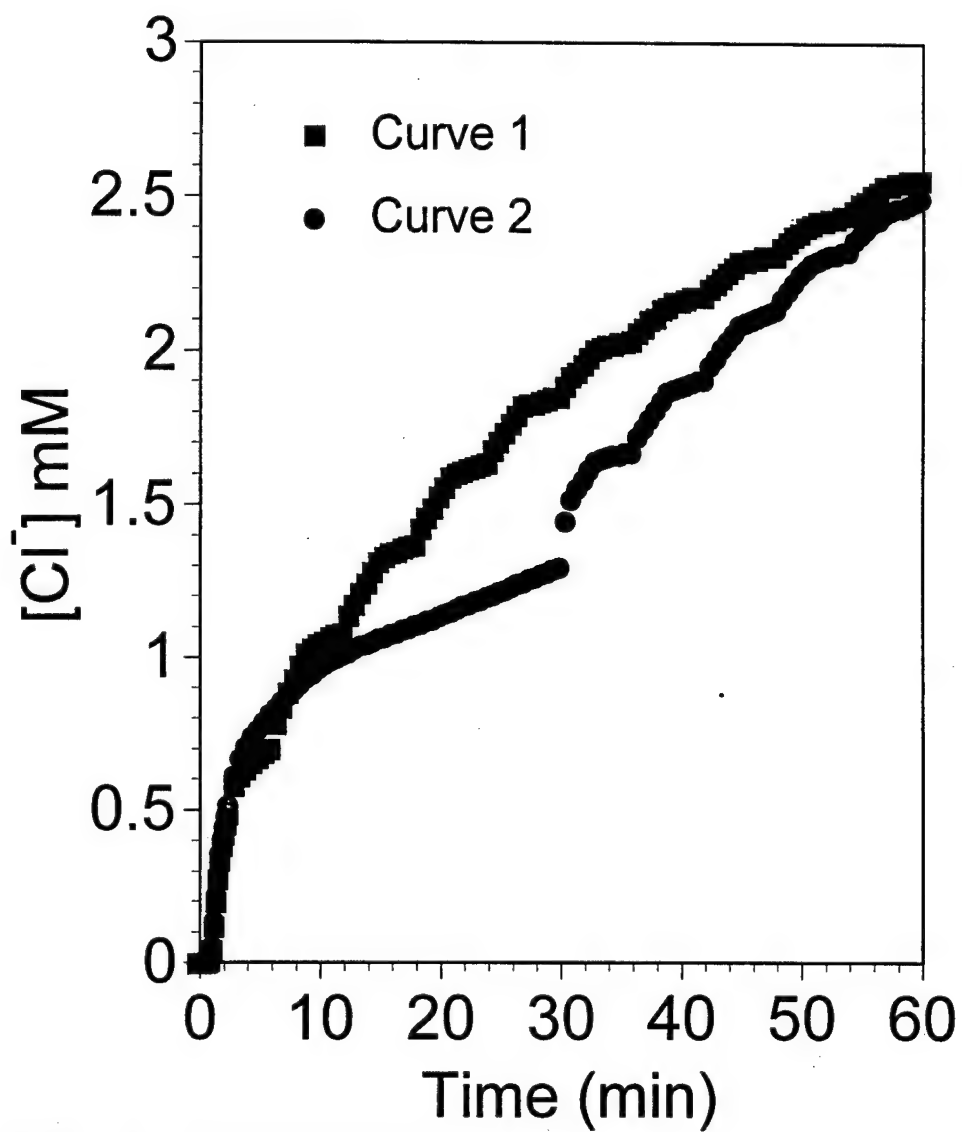
Figure I-11 Two post irradiation studies of 2 mL of R-11 in 110 mL of Ar-saturated, 0.5 g/L TiO$_2$, 0.30 M formate/formic acid buffer, and 7.0 x 10^{-5} M(hv)/min

are very low, these results clearly demonstrate that the propagation steps I-16 and I-17 are more efficient than the termination step I-18. irradiation processes induce smaller changes in [Cl⁻], they continue to occur even after long times, but at very low speeds. These results clearly demonstrate that the propagation steps I-16 and I-17 are more efficient than the termination step I-18.

Another interesting result is that at longer times the light-induced changes in [Cl⁻] approach those induced by the post irradiation process, that is, similar rates of Cl⁻ formation occur irrespective of the presence or absence of light. Figure I-12 shows the instantaneous rate of Cl⁻ formation for the light-induced and post irradiation processes as a function of cycle number. Here a cycle means one period of illumination plus the subsequent dark period, and the instantaneous rates are calculated from the steep and nearly linear increase of [Cl⁻] at the beginning of each period. Both the photochemical and dark instantaneous rates decrease with increasing cycles, but the decrease in the former is much larger. The convergence of both instantaneous rates at longer times not only implies that light turns out to be increasingly less efficient at initiating new chains, it also suggests that one or more products interferes with the initiating as well as the propagation steps.

Competition Studies

Experiments on the post irradiation effects show that both the photochemical as well as the thermal generation processes turn less efficient with increasing reaction time. Furthermore, given the amount of R-11 added and the amount of chloride produced, the yield of the Cl⁻ ions is less or equal than 10% even under continuous illumination. Thus, consumption of the starting material is not the cause for decreases in the reaction rate. Catalyst poisoning is a possible reason if products adsorb to the oxide surface. In order to test this possibility experiments were performed where Cl⁻, F⁻, and HCO_3^- ions were added to suspensions with 2 mL of R-11, 0.5 g/L TiO_2, 0.30 M formate/formic acid buffer that were degassed with Ar. Figure I-13 shows how [Cl⁻] changes during the induction period for these experiments while Figure I-14 is the corresponding plot for extended periods of time. As can be seen in Figure I-13, the presence of F⁻ (1×10^{-5} M) or Cl⁻ (5×10^{-5} M) has practically no effect on the induction period or on
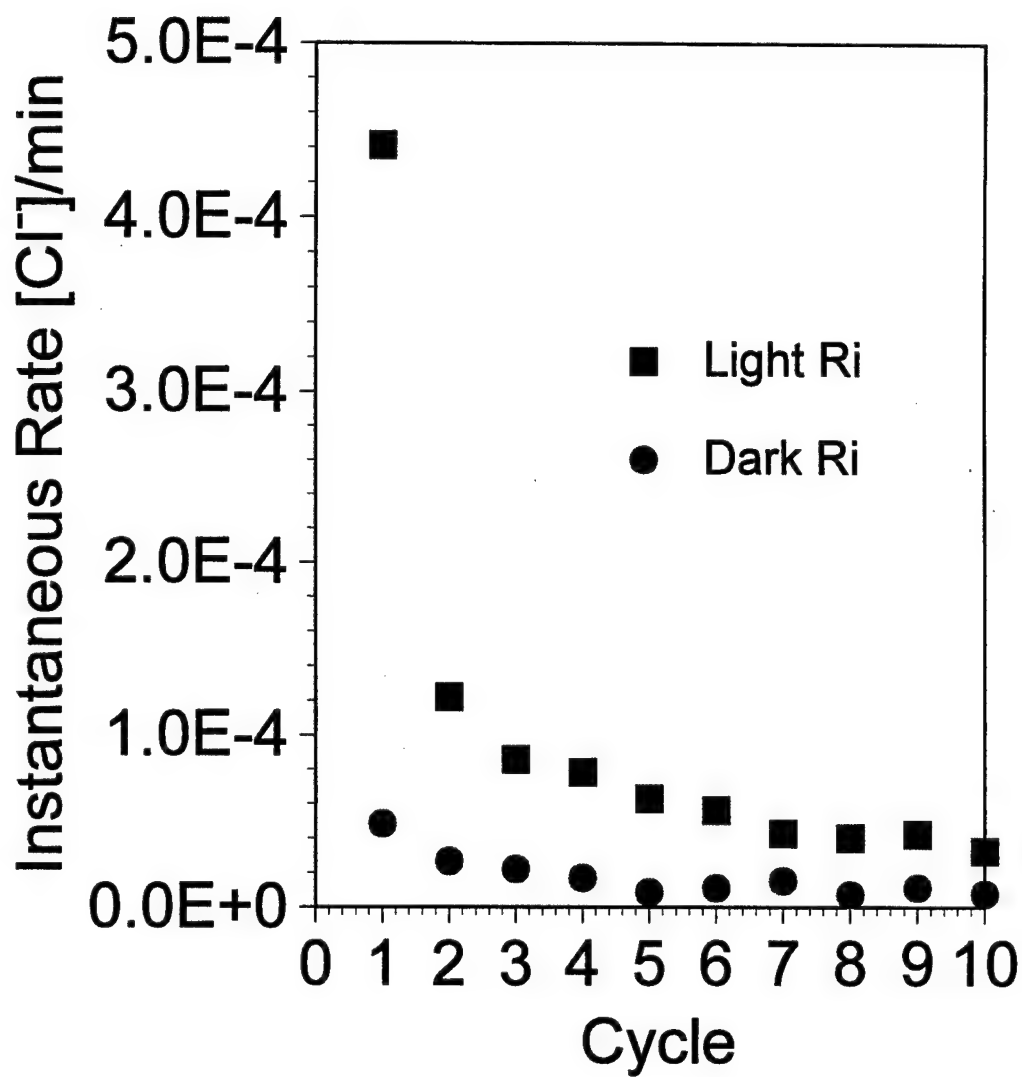
Figure I-12 Comparison of Photo and Dark reaction rates for 2mL R-11 in 110 mL of Ar-saturated, 0.5 g/L TiO_2, 0.30 M formate/formic acid, and 7.0 x 10^{-5} M(hV)/min.

Figure I-13 Chloride production of 2 mL of R-11 in 110 mL of Ar-saturated, 0.5 g/L TiO_2,

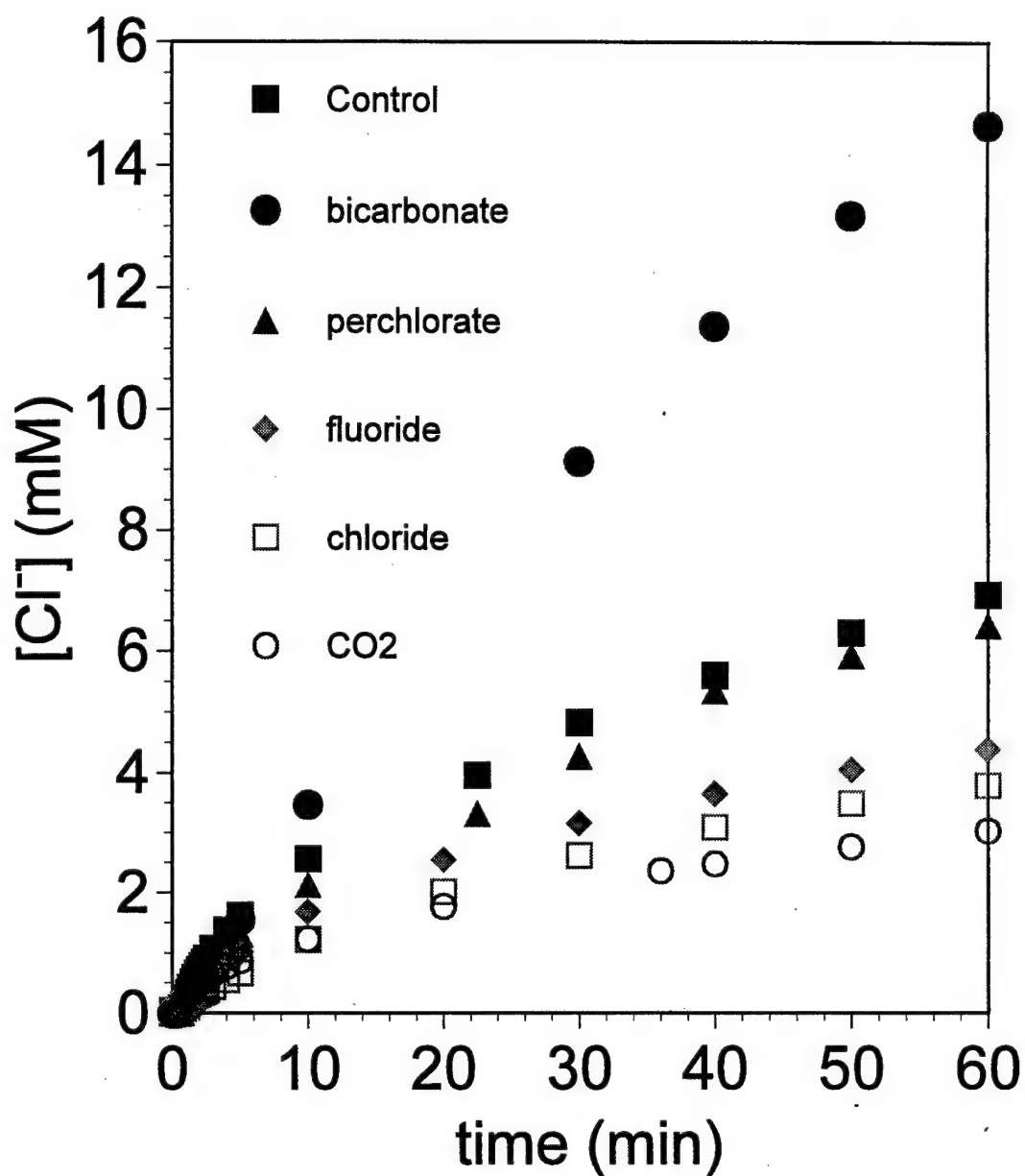0.30 M formate/formic acid buffer, 7.0×10^{-5} M(hv)/min and spiked with the
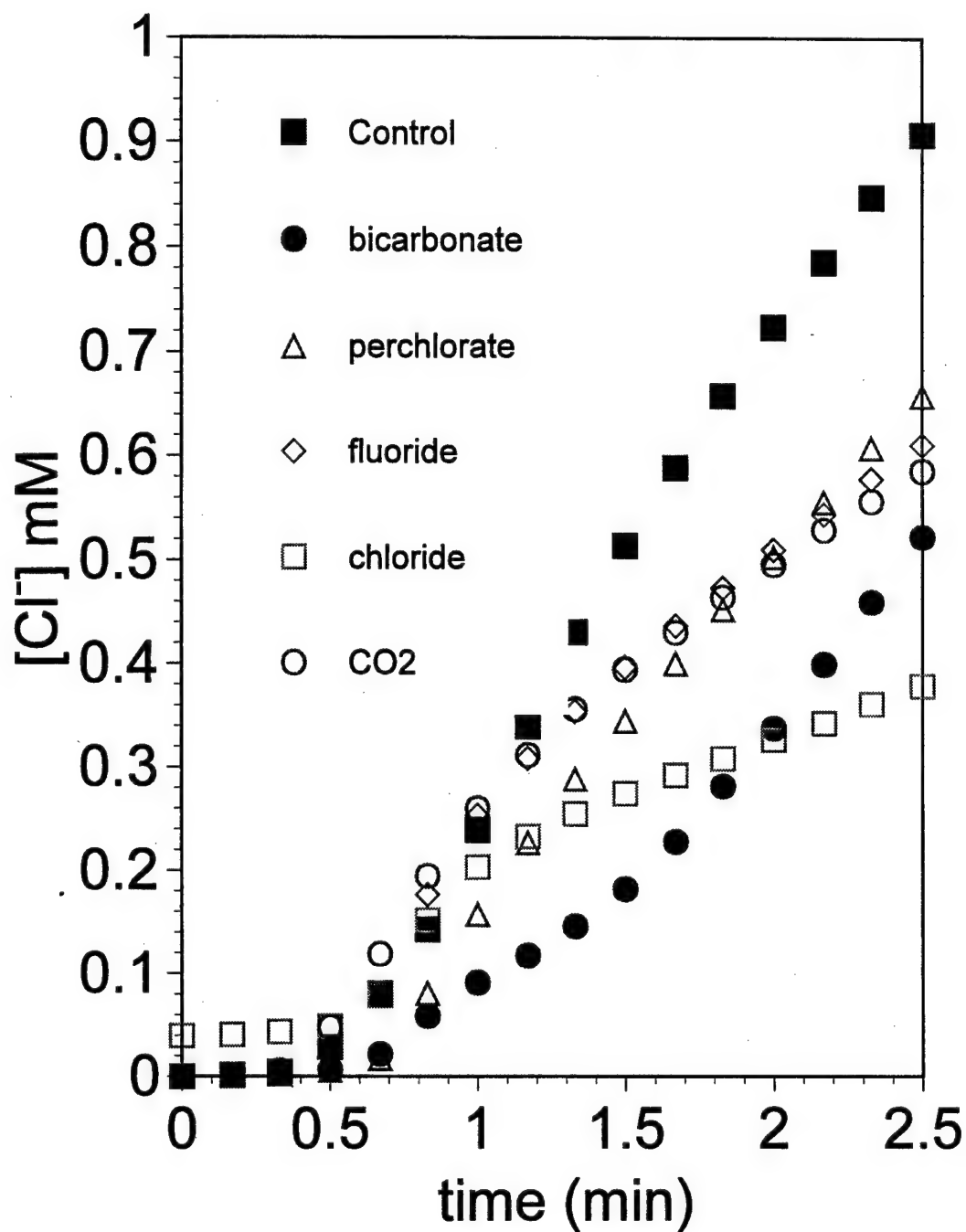indicated ion.

Figure I-14 Chloride production at short times of 2 mL of R-11 in 110 mL of Ar-saturated,

0.5 g/L TiO$_2$, 0.30 M formate/formic acid buffer, 7.0×10^{-5} M(hv)/min and

spiked with the indicated ion.

the initial rate of Cl⁻ formation during the fast step. However, the data of Figure I-14 indicates that at longer times, Cl⁻ formation decreases to about 50% of the value measured in the absence of initially added halide ions. A possible explanation is that adsorbed Cl⁻ and F⁻ ions act as recombination centers, lowering the amounts of reducing radicals available to attack R-11:

$$X^-_{(ads)} + h_{VB}^+ \rightarrow X_{(ads)} \quad (I-31$$

$$X_{(ads)} + e_{CB}^- \rightarrow X^- \quad (I-32$$
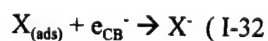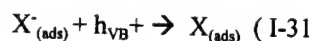
where $X^- = Cl^-, F^-$.

However, the occurrence of steps I-31 and I-32 is expected to increase the length of the induction period, which is not observed. Another possibility is that Cl⁻ and F⁻ ions present at or near the interface, that is, the ions present in the double layer, displace R-11 molecules and HCO_2^- ions. This is the most probable explanation to the data of Figure I-13 and I-14 because in chain processes, efficient propagation takes place only at very high reactant concentrations where propagation is very fast. In the R-11 system concentration decreases of CFC (and HCO_2^-) in the reaction zone have a negative influence on the propagation steps, lowering the rates of Cl⁻ generation.

Included in Figures I-13 and I-14 are results of experiments where 1×10^{-2} M $NaHCO_3$ or $NaClO_4$ were added to the suspensions. It is worth noting that HCO_3^- ions adsorb strongly and irreversibly to the TiO_2 surface,[28] whereas ClO_4^- ions do not.[29] Perchlorate ions induce a moderate inhibiting effect only at short times, probably due to the fact that these ions are present mainly in the double layer and are unable to displace freon molecules (and HCO_2^-) from the semiconductor surface.

Bicarbonate ions have a profound inhibiting effect extending beyond the induction period. However, after 10 min of illumination, the Cl⁻ yield is the same as in suspensions initially free of this chemical. Large increases of [Cl⁻] are detected at longer times in the bicarbonate system, leading to amounts of Cl⁻ generation that are twice as high as in the absence of HCO_3^- ions. The initial inhibition can be explained under the assumption that HCO_3^- ions efficiently displace formate and R-11 from the interfacial region, but displacement of the halide ion is more efficient. If that is the case, HCO_3^- will

eliminate, in part, the inhibiting effect of Cl^- ions in the reduction of the CFC. This, in turn, translates in more efficient chain reactions. Possible inhibitions due to the scavenging of holes or $^.OH$ radicals via:

$$HCO_3^- + h_{VB}^+/^.OH \rightarrow {}^.CO_3^- + H^+/H_2O \quad (I-33$$
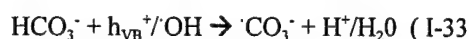
were not considered to be important since $^.CO_3^-$ reacts with HCO_2^-.[4]

$$^.CO_3^- + HCO_2^- \rightarrow HCO_3^- + {}^.CO_2^- \quad (I-34$$

to generate $^.CO_2^-$ radicals. Therefore, $^.CO_2^-$ radicals that may not form directly though reactions of h_{VB}^+ or $^.OH$ with HCO_2^-, will eventually be formed via steps I-33 and I-34.

Also presented in Figures I-13 and I-14 is the evolution of [Cl^-] in a suspension degassed with CO_2 instead of Ar. Rates of Cl^- generation similar to those of Ar-saturated suspensions are noticed in the presence of CO_2. At longer times, the rate of Cl^- formation is about 50% lower than in CO_2-free suspensions. It should be noted that no significant pH change was measured when 1×10^{-2} M HCO_3^- was added to the formate buffer. On the other hand, saturation of the suspensions with CO_2 is expected to exhaust the buffering capacity of the HCO_2^-/HCO_2H mixture. In fact, the pH of a CO_2 saturated aqueous solution is about 3.8, and lowering the pH of TiO_2 suspensions is known to decrease the efficiency of the photoreduction of R-113.[16] Therefore, we believe that a similar effect takes place in our system; studies on the pH dependence of ξ (Cl^-) will be performed in the near future in order to test our explanation.

Though not completely characterized, these results have certainly shown that the photoreaction of R-11 with TiO_2 with the use of a suitable hole scavenger is a chain mechanism of impressive efficiency. The mechanism presented is consistent with the results to date. Further inhibitor studies with the product, $HCCl_2F$, hydrogen peroxide, H_2O_2, other initial chloride concentrations, and pHs might perhaps yield the complete answer to the rapid decline of chloride production after the initial "explosion".

II. PHOTOREDUCTIONS OF HALOMETHANES IN AQUEOUS, CONVERTED, POLYACRYLONITRILE (CPAN) FIBER SUSPENSIONS.

Background

The thermal treatment of PAN to form carbon fibers has been well studied since the 1960's. This conversion, however, is not a one step process. PAN exhibits variable properties at different points along the transformation from a white, somewhat delicate polymer fiber, to graphite at the end of pyrolyzation. As the transformation proceeds, PAN becomes tough, and changes color to yellow and eventually red. This process was characterized in 1967 by Friedlander et al. as the formation of, "...partially hydrogenated naphthyridine-type rings produced by linking up of adjacent nitrile groups."[30] Further optical data was provided by T.-C. Chung et al. in 1984.[31] The scheme by which PAN is converted is shown in Figure II-1. This type of polymer having conjugated double bonds is similar to other known organic semiconductors.[32] Consequently, this work was begun with the idea in mind that PAN could serve a dual purpose: a fabric for clothing that also has semiconductor properties.

Commercial PAN fabric was converted into the conjugated polymer and then ground to a consistency approaching a powder. To explore possible semiconductor characteristics, an optical reflectance spectra was obtained using an integrating sphere. Figure II-2 shows the resulting spectrum. The band-gap may be obtained by noting the inflection in the raw data, or a peak in a derivative spectrum (Figure II-3).[33] For converted PAN (CPAN) a band gap of 2.2 eV is obtained. For comparison, the first derivative of the reflectance spectrum of TiO_2 in presented in Figure II-4. The validity of the
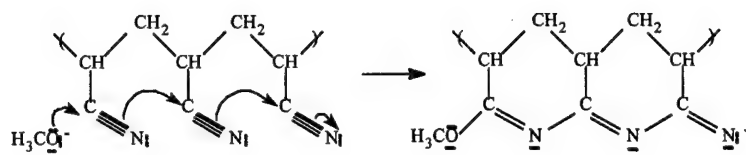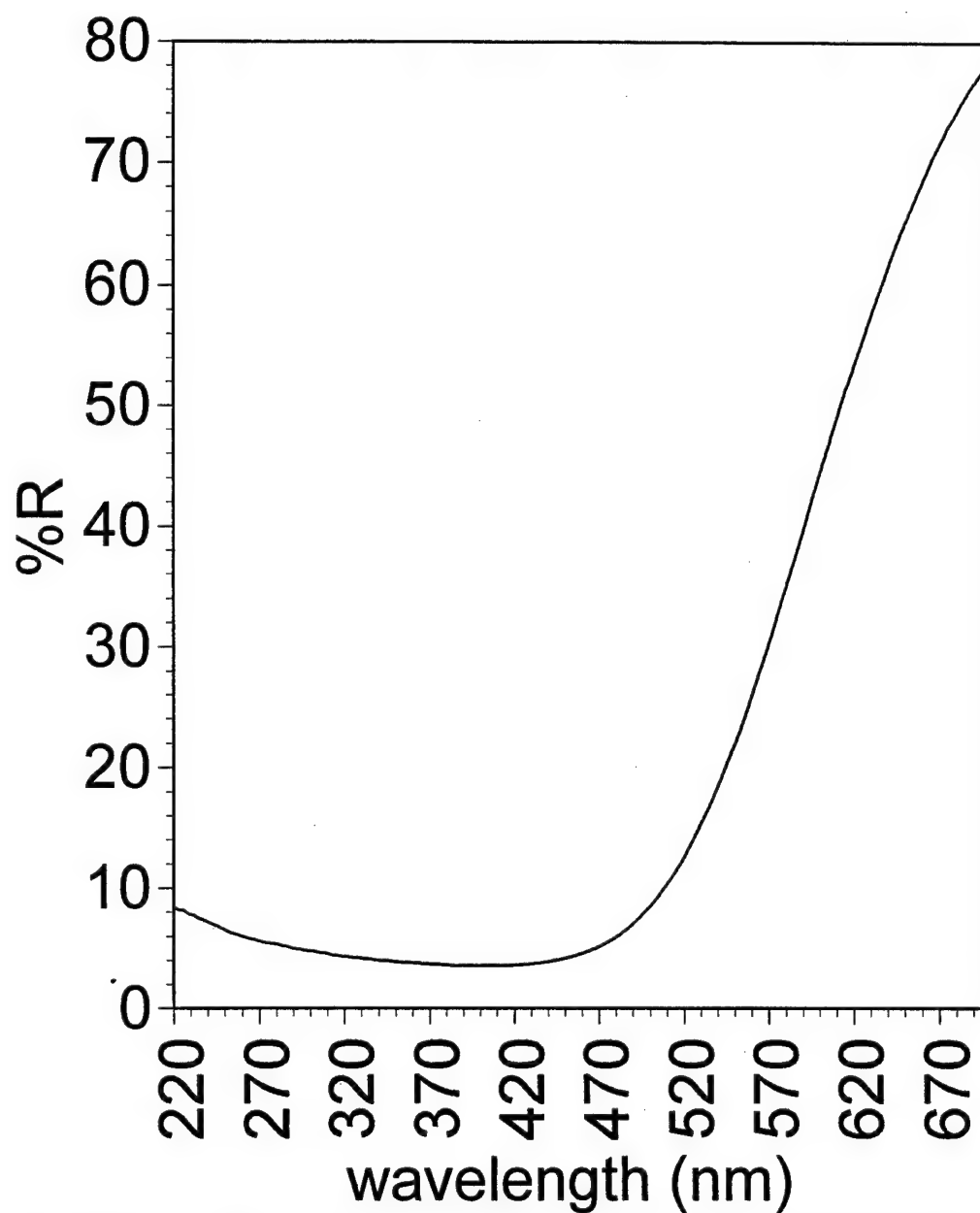
Figure II-1 PAN conversion mechanism.[36]

Figure II-2 Optical reflectance spectrum of ground CPAN derived from the commercial fabric
Creslan treated with 0.01M NaOCH$_3$ for 3 minutes at 150°C.
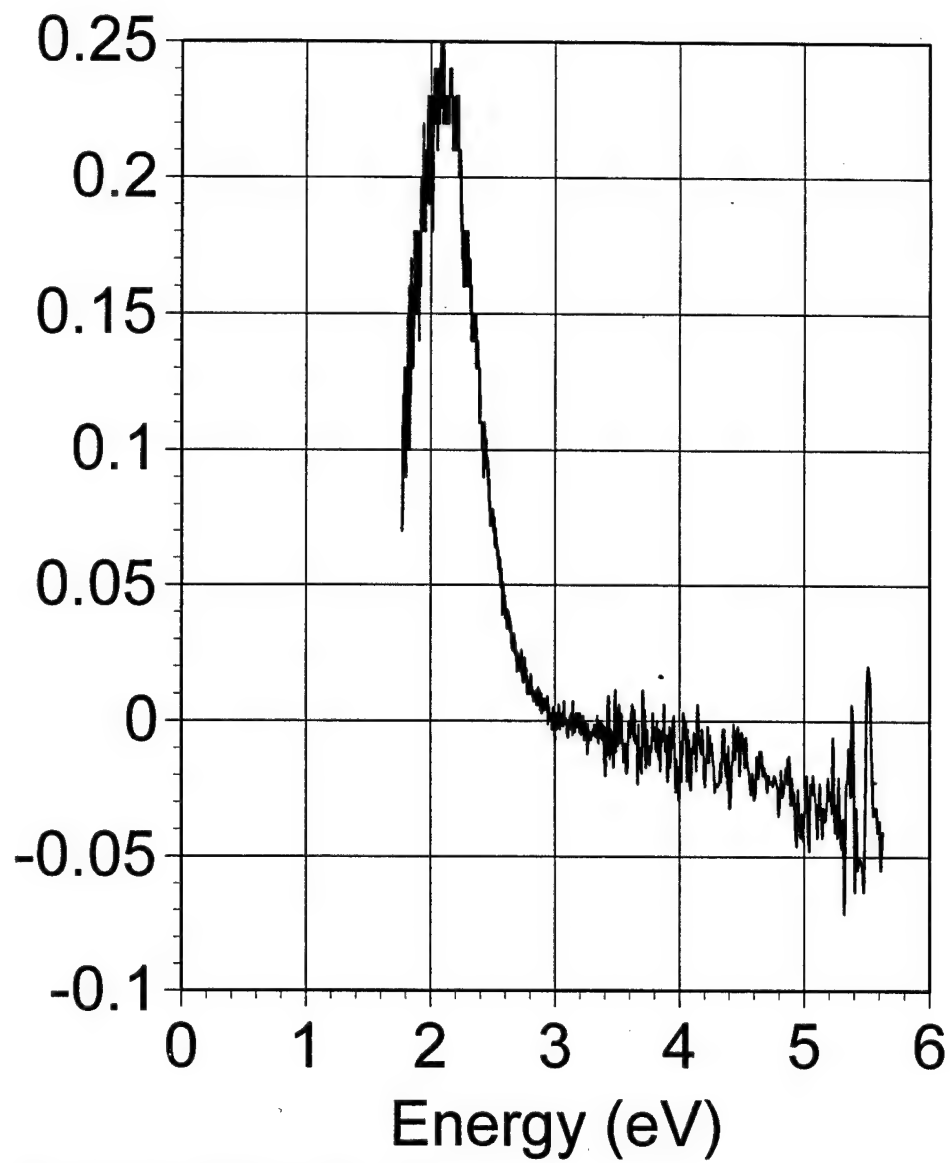
Figure II-3 First derivative of Figure II-2
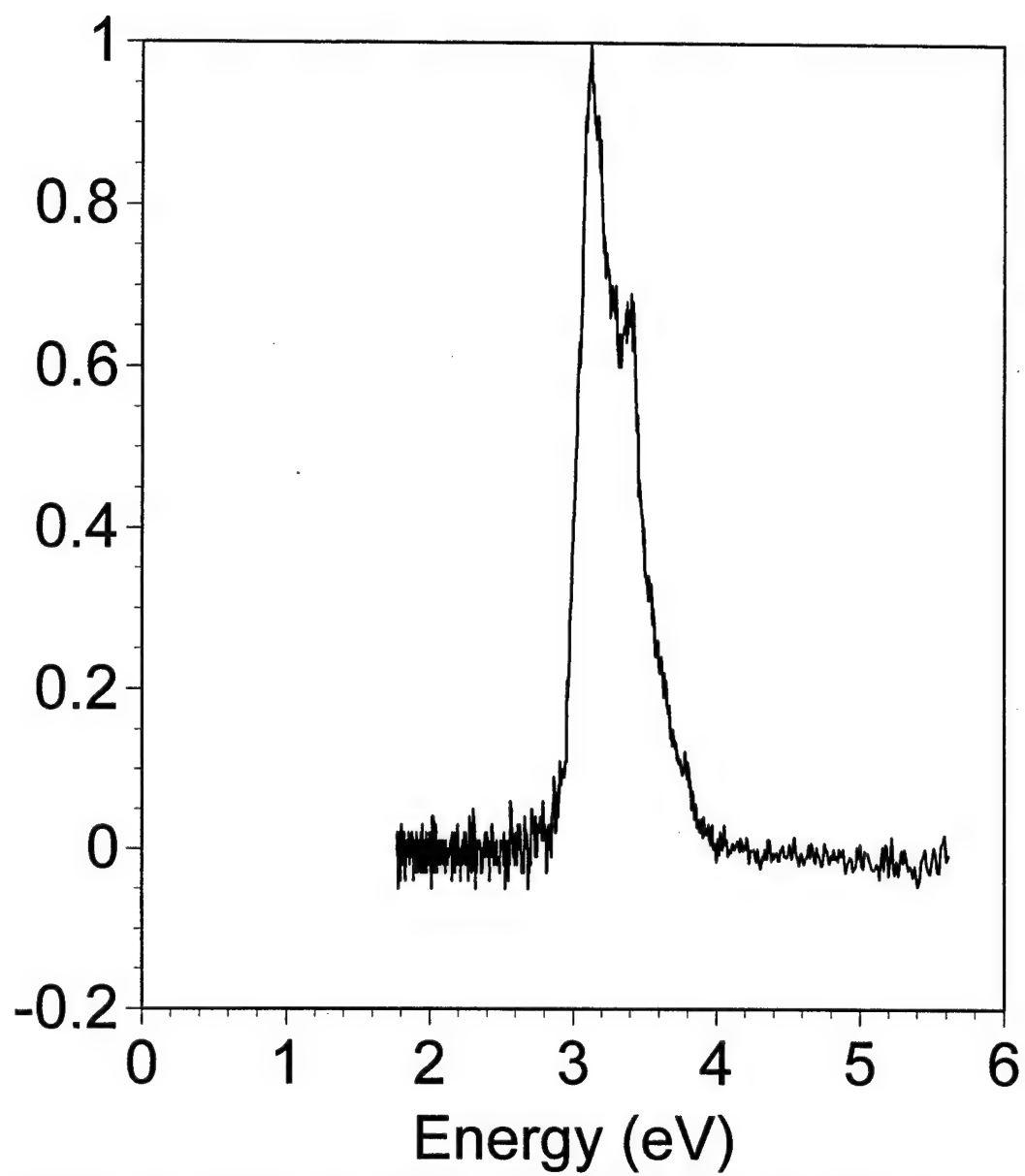
Figure II-4 First derivative of the reflectance spectrum of Degussa P-25 used in chapter I.

method was tested by analyzing TiO_2 P-25, consisting of two semiconducting phases rutile and anatase. Band gaps of 3.1 and 3.3 eV are obtained respectively which agree nicely with their respective reported values.[14]

Based on the ability of some semiconductors to induce phototransformations of chemicals in the presence of UV light as was shown in chapter I, this same type of scheme was pursued using CPAN. Aqueous suspensions were subjected to light after the introduction of a halomethane. Early experiments were run with chloroform which is a relatively non-toxic model for nerve agents. Later reactions were attempted with R-11. The cursory initial results are presented here.

Experimental

The commercial PAN fabric used was Creslan Acrylic and was washed consecutively in hot deionized (MILLIPORE) water, hot methanol, and hot cyclohexane. The fibers were allowed to dry at 50°C in air overnight.

125 mL of 0.1M $NaOCH_3$/ethylene glycol was prepared and heated to 150°C. A sample (3g) of the cleaned fabric was stirred in the above solution for 17 minutes (the fabric had turned from white to dark red). Upon removal, fabric was rinsed in 3 half liter batches of house distilled water and a final rinse in 1L of DI water. The samples were then dried for ten days at 50°C in air. A weight increase of 8% was detected after the treatment.

After results of experiments with this fabric, a milder conversion was deemed necessary. The second method employed a 0.01M solution of base and treatment lasted only three minutes. This resulted in a dark yellow fabric that had a 10% weight increase.

Fabric was ground using a ½ h.p. mill. Size filter screens were used in an attempt to obtain a consistent particle size. The fabric exhibited too much clumping, however, and the screens were merely

clogged. It is estimated the size is in the tens of microns range. CPAN was added to the reactor vessel and the experiment conducted similar to that in chapter I.

CPAN reactions were run with sodium perchlorate to ensure the activity of the solution was as close to 1 as possible. The solution was 100mL of DI water that was 0.1M in perchlorate and contained 1.02g CPAN. Degassing was accomplished using N_2 (AIRCO) for 45 minutes.

Chloroform, CH_3Cl (FISCHER A.C.S.) was washed three times with DI water (MILLIPORE) and stored in the dark with 250mL of DI water on top. Prior to injection to the reaction, air was removed via the freeze, pump, thaw method.

Early experiments utilized a 3-75 filter (KOPP), while later reactions were run with the 7-60. Reflectance spectra were obtained via a model 2501 UV-Vis spectrophotometer (SHIMADZU), equipped with a model ISR-2200 integrating sphere.

Results and Discussion

This reaction proved far more difficult to characterize than the TiO_2 system. The most difficult problem was the inability to successfully rid the fabric of excess base (probably methoxide ions). This anion hydrolyzes in water to form methanol as follows:

$$OCH_3^- + H_2O \rightarrow HOCH_3 + OH^- \quad (II-1$$

The problem with this reaction is that hydroxide ion causes interferences in the detection of Cl^- (an expected product of the transformation of $CHCl_3$). Hydroxide ions alter the nature of the AgCl material employed for the detection of Cl^-:

$$2AgCl + OH^- + H_2O \rightarrow Ag_2O + 2HCl + OH^- \quad (II-2$$
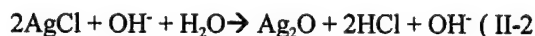
The solubility of the oxide is only 14 times more than the chloride, so this is definitely significant.

Reactions with chloroform/perchlorate

The first reaction run used fabric that had undergone conversion using 0.1M methoxide and was thus very dark. Addition of 1g of CPAN to the perchlorate solution resulted in a change from 117 mV to 217 mV. This would correspond to a production of 1.5×10^{-4} mol of Cl^- without ever adding CH_3Cl or turning the light on. An experiment revealed that heavily treated CPAN raised the pH of water from 5.4 to 8.6 over the course of a day. Obviously, this was unsatisfactory. To verify the hydroxide interference, 1.4×10^{-3} mol of methoxide was added to a blank perchlorate solution. This amount of methoxide corresponded to the maximum amount of methoxide possibly in the fabric based on its weight change. A voltage change of 70 mV followed.

The first attempt at a remedy was using milder treatment conditions for the fabric. The base concentration was lowered by an order of magnitude and the treatment time reduced by ¾. A more detailed experiment was then performed. First, the pH was measured for 100 mL of DI water with the result being 5.3, which results from dissolution of CO_2 (from air) into deionized water. Upon introduction of 0.1 M $NaClO_4$ the pH was 6.3, and voltage readings between 137 and 127 mV.

A photoreaction using this more mildly treated fabric, showed favorable, albeit slow, results showing changes in potential vs. time are presented in Figure II-5. Another reaction was run in excess of 15 hours with what appeared to be 0.4 mM Cl^- produced. With good results in hand, another patch of fabric was converted via the same mild method in order to run a blank. All preparation was the same except no chloroform was added. A steady upward voltage drift of 30 mV over 250 minutes occurred, which was well in excess of that seen in the previous reaction thought to produce chloride. Even more puzzling was that this drift was linear as opposed to the classic induction type reaction seen previously. Hydroxide was the assumed problem, so attempts were made to remove the base by treating with acid. In fact, perchloric acid equal in concentration to the base added to convert the fibers, was used to wash the
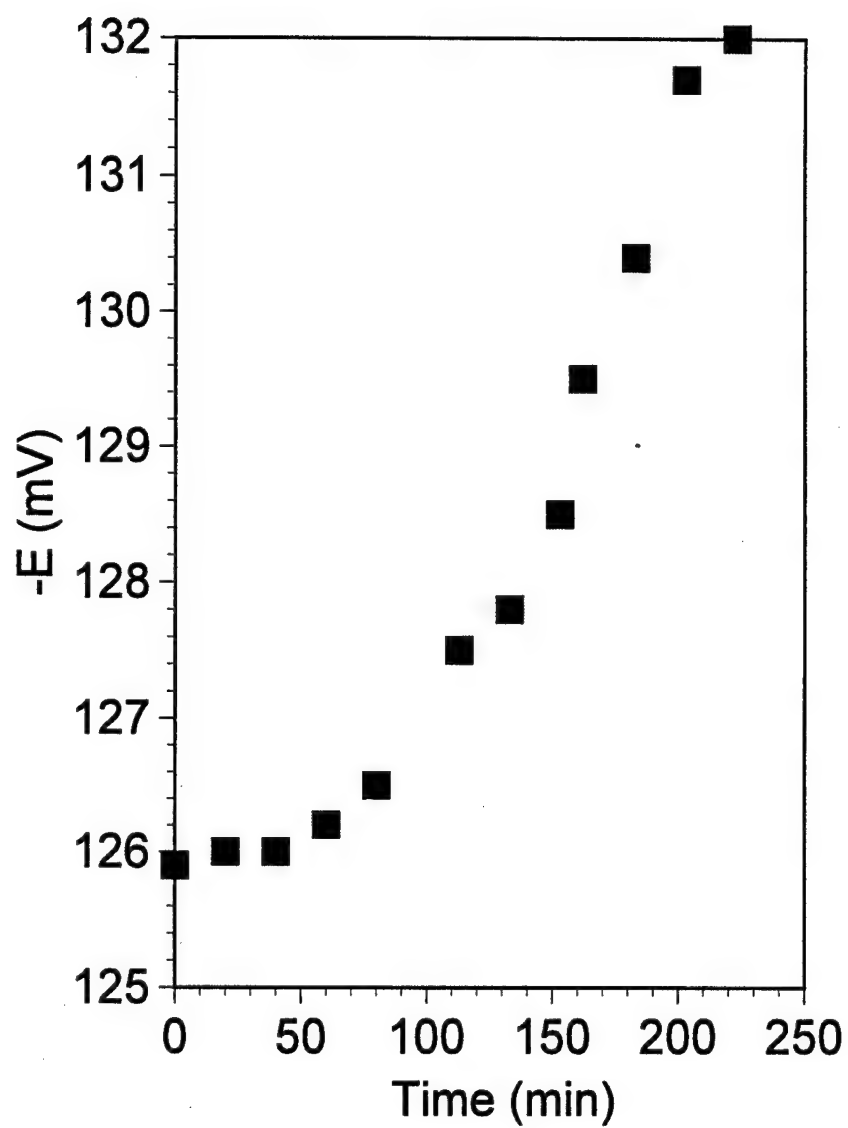
Figure II-5 Reaction of 0.25 mL of chloroform in 100 mL of 0.1 M
perchlorate and 0.767g of CPAN shown in Figure II-2.

fabric overnight. This fabric was then rinsed with two ½ L aliquots of DI water and the blank rerun. Results again showed drift.

As one last check before this line of investigation ended, the filtered solution from the reaction of Figure II-5 was treated with AgNO$_3$. As is typical in making AgCl at low concentrations, the solution first turned white and cloudy over the course of a day, then turned dark over the course of a week. Attempts to isolate enough precipitate for x-ray analysis were unsuccessful.

Reactions with R-11/formate

Based on previous success of Weaver et al. with a freon/formate system,[30] experiments with CPAN were made along these lines as well. It is known that the reduction of CH$_3$Cl to form chloride ions is quite difficult, but chapter I has shown R-11 to be readily accessible. The hope was that this system would produce a great deal of chloride such that the OH$^-$ drift could be subtracted. Prior to this reaction, the mildly treated CPAN was rinsed overnight in pH 1 DI water in an effort to neutralize all the base. The blank run with this fabric was promising in that the drift was only a few millivolts over 8 hours. To further explore the effects of the rinsing solution, a blank was run with a slightly transformed fabric rinsed only in several batches of DI water. Both blanks contained 0.1M formate and were run in 100mL of DI water. These are compared in Figure II-6. As can be seen, the effect of the rinse solution makes a marked difference in the amount of interference ions leached from the fabric.

With these results in hand, the fabric rinsed at pH = 1 was used in a photoreaction with R-11 and formate ions. Results are shown in Figure II-7. The correction applied stems from the drift seen in the blank shown in Figure II-6. Simple subtraction of the maximum "chloride" concentration seen in the blank from all data in the reaction results in the corrected data shown in this figure. Thus, finally, a procedure for treating the CPAN was successful at eliminating some of the interferences to levels that are tolerable in investigation on the photochemical properties of CPAN.

This reaction is certainly different from those seen in chapter I. First, there appears to be no induction period. Chloride production appears to follow a zero-order rate throughout the first 200 minutes. Secondly, there is no "explosion" of chloride after an initial slow rate. Though no light intensity measurements were made for these samples, previous experience with the light intensity and the reactor vessel used in this investigation indicates that ξ (Cl-) values are <<1. All these pieces of evidence suggest no chain mechanism operated in this system. However, the intent of the study was find out if, in fact, CPAN could initiate photoreductions similar to those triggered by TiO_2. In that respect, the experiment was successful. Further investigation is warranted so that conditions may be found that would significantly increase the efficiency of this photoreaction.
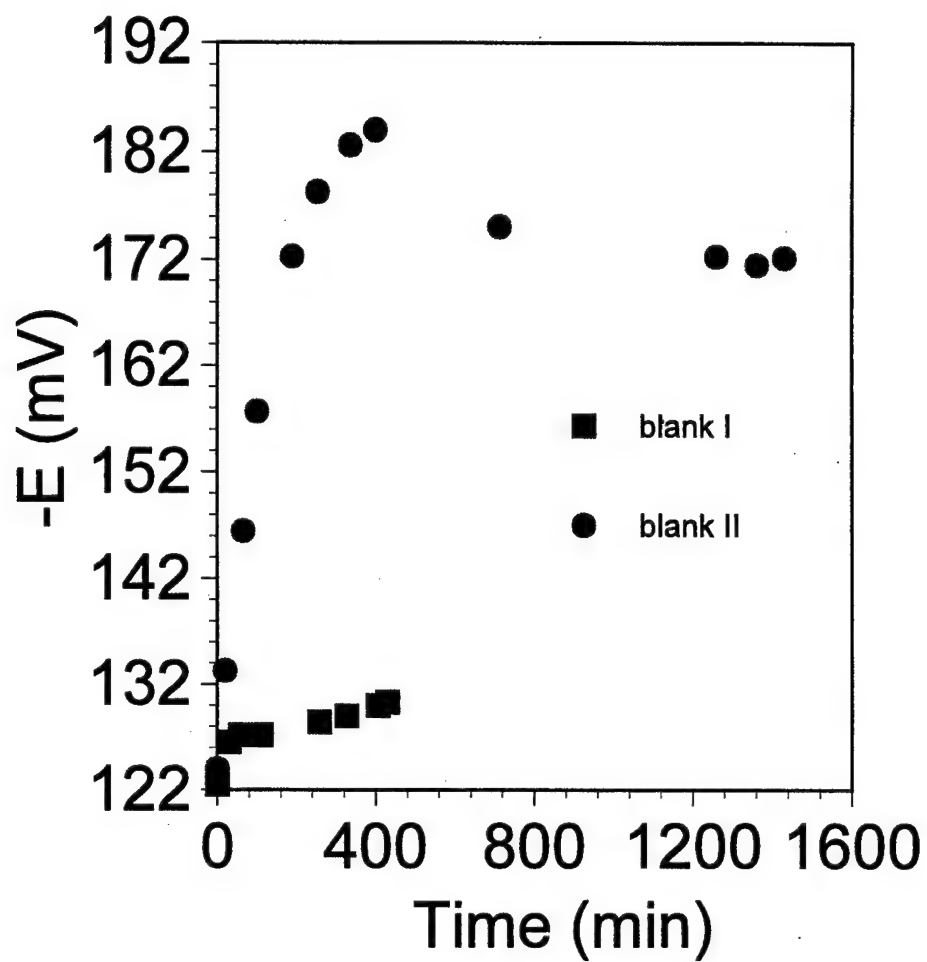
Figure II-6 Comparison of the voltage drift induced by 0.75g of
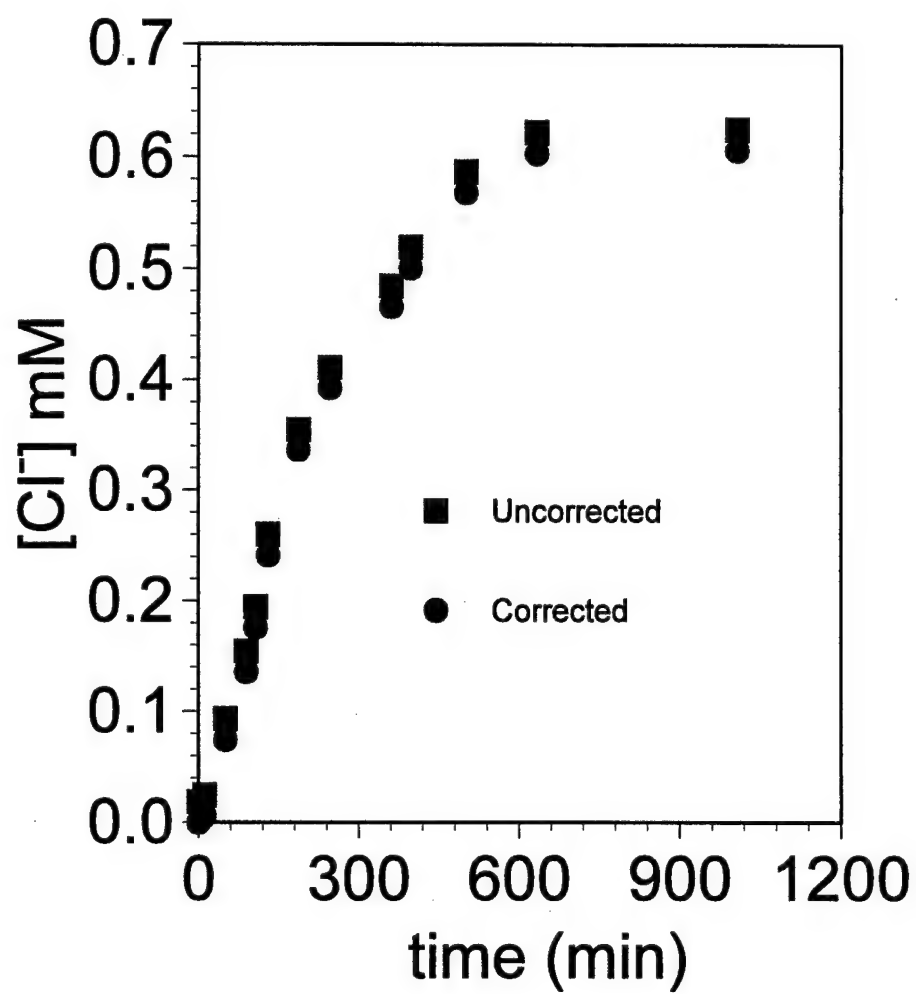pH3 and pH1 rinsed CPAN in 110 mL of 0.1M formate
solution.

Figure II-7 Reaction of 1.4 g of pH1 rinsed CPAN with 0.3 mL R-11 in
110mL of 0.1M formate

III. ELECTRICAL AND OPTICAL CHARACTERISTICS OF THIN FILMS OF CONVERTED POLYACRYLONITRILE (CPAN)

Background

As discussed in Chapter II, treatment of PAN with methoxide ions induces color changes of the polymeric fibers. These changes are suspected to arise from a transformation of insulating PAN into a semiconducting material, where the different colors correspond to changes in the band gap of CPAN. Organic semiconductors based on CPAN are expected to offer significant advantages in terms of device fabrication because complex structures can be first made out of PAN, followed by subsequent conversion to one or more semiconducting phases. However, physical properties of semiconductor are easier to study for materials present as films. Also, films lend themselves to portable applications much easier than fibers because much of the current electronic technology is based on film structures. Presented in this chapter are results from studies on optical and electrical properties of CPAN films.

Although various methods of organic film growth are available, most effort has been spent forming them via Langmuir-Blodgett methods or self-assembled monolayers.[35] However, these methods require molecules that are easier to orient. However, orienting PAN molecules has proven to be a difficult task, in fact, solid PAN seems to exhibit a variety of crystallographic phases which are formed by inclusion of varying amounts of solvent molecules in the solid lattice. Thus, two other avenues of approach needed to be examined. Spin and solvent casting are really just two different means to the same end, that is, to rid the polymer of a sufficient amount of solvent to make it behave as a solid. Both of these methods were explored.

For the purposes of this work, a satisfactory film should have several characteristics. First, it has to be transparent in order to be useful for optical determinations. Other methods became available very late in the study which allowed measurement of an opaque film, but that was an exception. Secondly, the film needed to be resilient. Possible applications would require the film to be handled and, in order to obtain electrical measurements, the film had to be placed in the somewhat hostile environment of a electron beam-metal deposition chamber. Finally, in order to handle the film for the above purposes, it had to adhere to a substrate. Hence, the first task was to develop procedures for the preparation of films with the above mentioned mechanical and optical properties.

Experimental

Thin PAN fibers (90-92% acrylonitrile, 7.4-9.4% methyl acrylate , 0.6% sodium methallyl sulfonate) obtained from CTU(PRC), were soaked overnight in methanol, and dried in a vacuum oven. The dry fibers were then dissolved in DMSO at 90°C in a ratio of 0.02g PAN/mL. This solution was pale yellow. Two different treatment schemes were used to convert PAN to the cyclized form.

Films characterized as moderately treated were cast from a solution prepared by mixing 10ml of PAN solution and 20ml of 0.015M sodium methoxide in dimethyl sulfoxide at 60°C. This solution was stirred for 1hr before cooling under N_2. The result was a dark amber solution.

Films characterized as heavily treated were cast from a solution prepared by adding 0.038 g solid sodium methoxide to 11.9 mL of the 0.02 g/mL PAN solution in DMSO at 60°C. A very dark red solution appeared in less than five minutes. This solution was also cooled under N_2. Films characterized as untreated merely involved taking the 0.02 g/mL PAN/DMSO solution and casting via the method outlined below.

Another treatment scheme involved taking dried fibers and heating them in a 1M solution of sodium methoxide/ethylene glycol. These fibers underwent successive washings in DI water until the pH

stabilized at 5.2. After drying, 0.2 g of these orange fibers were placed in 20ml DMSO and stirred for one week at 60°C. The fibers proved to be sparingly soluble, but the resulting light amber solution was used to cast films characterized as washed.

The above solutions were used to solvent cast films on Fischer quartz microscope slides cut to 2.5 x 2.5 cm. The substrates were cleaned in hot isopropyl alcohol, rinsed in DI water, and dried in an oven at 100°C. To cast, each slide was covered by 0.5 mL of the appropriate solution and placed in a vacuum oven at 60°C for one hour. Films were completed by repeating this procedure three more times and cooling under N_2. UV/Vis Spectra were taken with an Hitachi 2000 or Shimadzu UV-2501 spectrophotometer.

Films were then taken to the Alabama Microelectronics Center where 32 mm circular gold contacts were sputtered through an aluminum mask. The contacts were laid down at 0.2 angstroms/min for ten minutes. Heavily treated films were somewhat brittle and showed some cracking. All other films were stable to this procedure. Two-point-probe resistances were measured corner to corner with an HP 5501 semiconductor analyzer with tungsten probes. Plots shown are the average of the two measured values. Half of the samples were measured by the Auburn Physics Department.

Results and Discussion

Production Method

Spin casting was attempted by utilizing various spin rates, PAN solution concentration, and amount of solution placed on the slide for each successive coat. No satisfactory films were produced. In general, too much solvent was removed too quickly and upon drying, brittle films resulted. The amount of solvent that remained in the films has important consequences to the film characteristics. Solvent casting proved a more reliable method of ensuring reproducible amounts of DMSO in the films.

Successful solvent casting resulted only after finding the correct mix of oven temperature, PAN solution concentration, and degree and method of base treatment. Temperature from room to 100° C were

utilized. Above 100° C, pyrolyzation begins to occur with graphite being the eventual product. PAN solution concentrations of 0.02, 0.04, and 0.08g/mL DMSO were all used, but the first concentration yielded the best results. Base treatment methods varied even more. To accomplish the cyclization, hot PAN solution was added to various concentrations of hot methoxide solution, solid base was added to hot PAN solution, and PAN and methoxide solutions were added to a slide and allowed to reaction in the oven during film formation. Optimization of all these factors proved that film making requires just as much art as science.

Film Physical Characteristics

Films made with more concentrated amounts of PAN became brittle over time. This results from a deviation from an ideal PAN/DMSO ratio left on the slide after solvent evaporation in the vacuum oven. To test this theory, successfully cast films were washed with water which is a solvent for DMSO but not PAN or CPAN. Upon drying under N_2, the films became very brittle, cracked and separated from the substrate in a manner similar to the more concentrated films. This effect was also seen in films of CPAN treated at temperatures above 100° C. This phenomenon also occurs in untreated films but manifests itself in being opaque instead of brittle. This also confirms that CPAN is fundamentally different than PAN.

Another treatment scheme that resulted in brittle films was the addition of solid methoxide to hot PAN solution. The methoxide was added such that the concentration would be the same as those prepared by mixing two solutions. Though the transformation is very fast by adding solid, the film quality is poor. Sodium methoxide is not overly soluble in DMSO, so the poor quality is probably due to undissolved base left in the film, which would change the CPAN/DMSO ratio. This method also produced films whose signal to noise in voltage measurements was very poor.

A third treatment scheme resulted in a very interesting film. First PAN fibers were converted in 50 mL of 0.1 M $NaOCH_3$/ethylene glycol at 60° C for one hour. The fibers were then washed in three half

liter aliquots of DI water to rinse out the base. Then the fibers were dissolved as much as possible in 50 mL of DMSO at 60°C. Previously converted fibers are much less soluble than the unconverted fibers. Annealing took place as usual. This film had mixed patches of dark amber CPAN and white opaque unconverted PAN. Unwashed films do not exhibit this characteristic because the annealing process promotes more conversion if base is present. This was tested by making films simply by placing drops of PAN and base solution together on a substrate and placing directly in a vacuum oven. Amber films resulted but, when held against a dark background, tiny specks of undissolved base could be seen with the eye.

Optical Spectra

Figure III-1 is the UV transmission spectra an acceptable film. Notable features include the shoulder at 358 nm and another large peak at ~280 nm. Figure III-2 helps to sort these features out. The peak at 358 nm is noticeably absent from the untreated film, indicating that this peak corresponds to modified PAN. It is also interesting to note that untreated PAN still exists in the treated film. Figure III-3 is shown to gain information about the bandgap of films compared to the fibers of chapter II. Note that since these are transmission spectra, the peaks analyzed are actually negative peaks. The shoulder which corresponds to CPAN yields a bandgap of 3.0 eV and the second (PAN) peak is the very large 4.5 eV. These are in excellent agreement with previously published data for pyrolyzed films.[36]

This value for CPAN film is different than that obtained in chapter III for the fabric. This is attributed to the extreme differences in the two different conversion methods. The fabric was converted at 150°C whereas the solution from which the films were cast was converted at 60°C and the films annealed at 60°C. Other possible sources of difference are the co-polymers present in each.
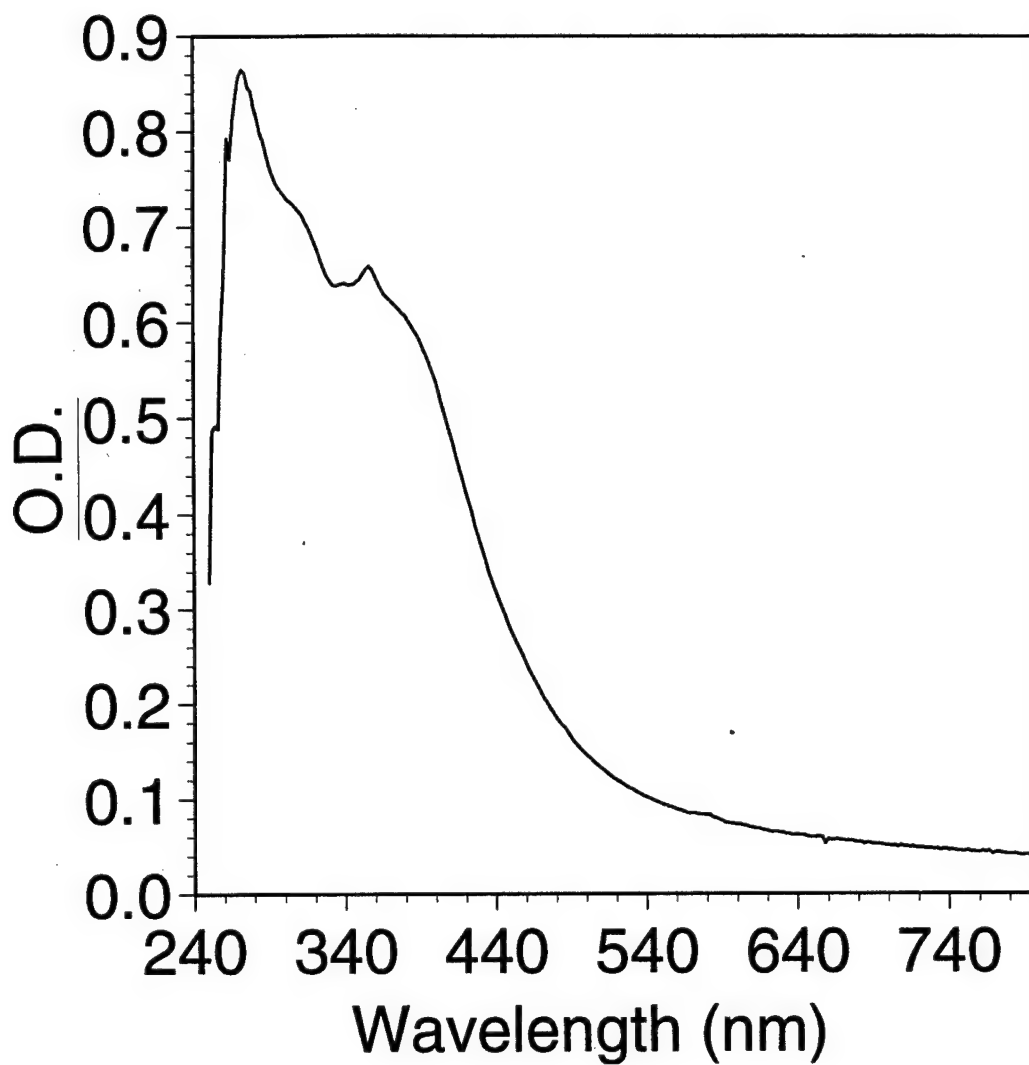
Figure III-1 Optical transmission spectrum of a CPAN film made from 20mL of 0.02g/mL PAN/DMSO solution treated for one hour at 60°C with 10 mL of 0.1M NaOCH₃/DMSO.
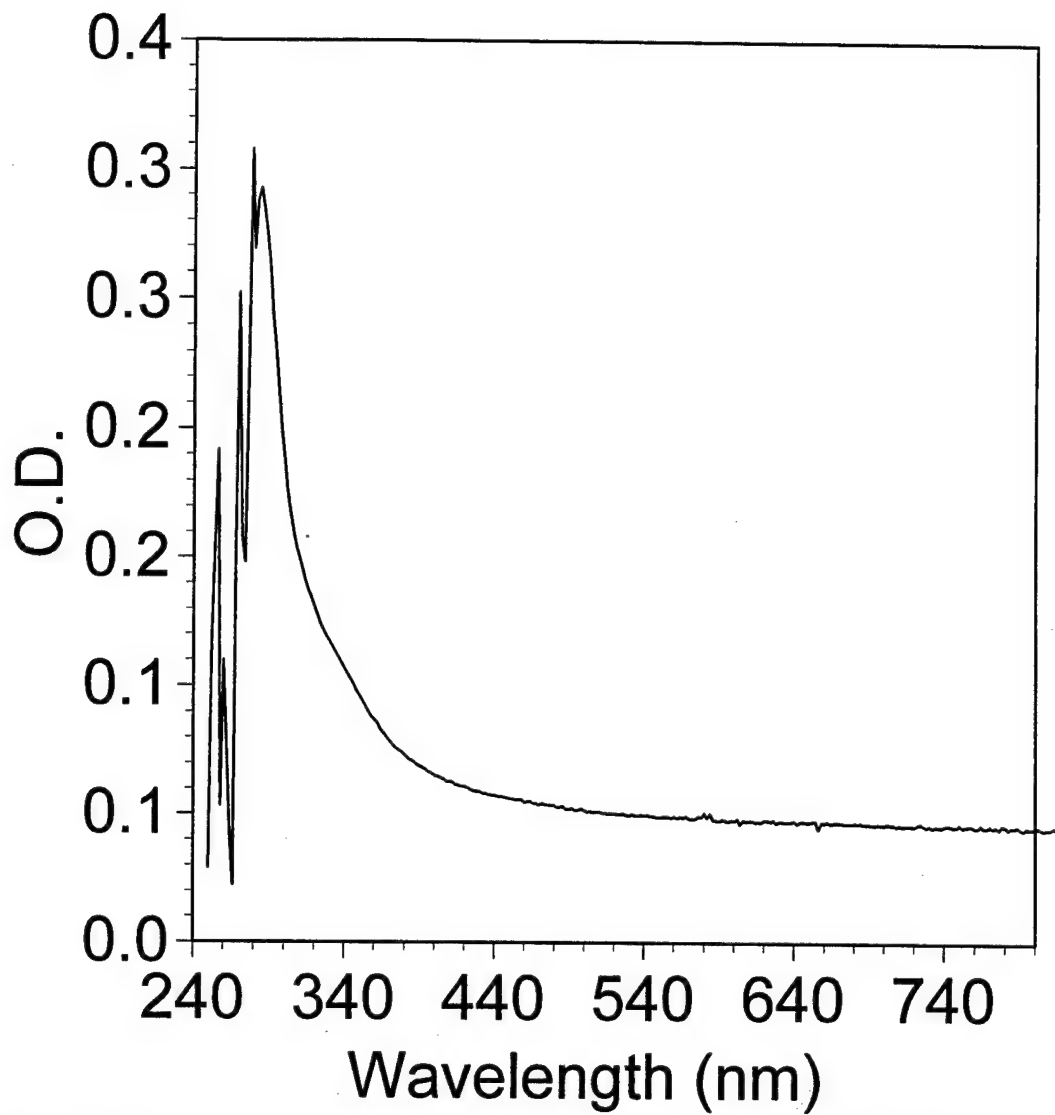
Figure III-2 Optical transmission spectra of an unconverted PAN film made from 0.02g/mL PAN/DMSO solution
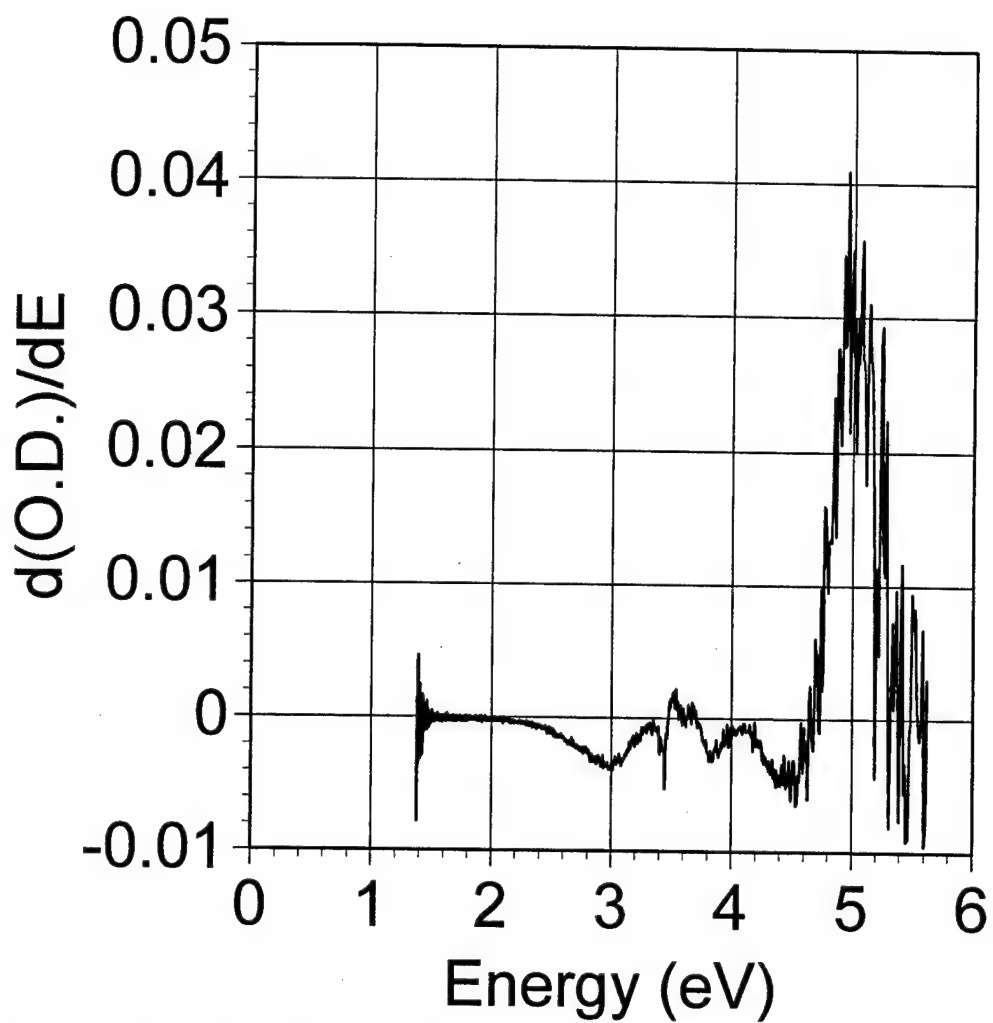
Figure III-3 First derivative of Figure III-1.

Figure III-4 shows a somewhat different spectrum. Reflectance is used because the film is opaque. Since it was made from a washed fiber film, it was used for comparison purposes. To properly interpret the spectrum vis a vis transmission spectra, turning the image upside down may help. One can see both peaks are present, but the peak associated with CPAN is much weaker compared to the PAN peak in previous films. The derivative of this spectrum shows no significant information until above 4.5 eV which further supports this films composition as mostly PAN.

<div align="center">Resistance measurements</div>

Figure III-5 is the two probe results for the film shown in Figure III-1. Note there is essentially no hysteresis which indicates the contacts have ohmic behavior [37] and it is evident that the signal passes through the origin. The measurement was made in the presence of light close to the sample and just background room light. The only difference between the two was more noise in the closely lit sample, thus CPAN does not appear to be a photoconductor. Note also the linearity of the plot showing that the contacts are ohmic and a resistance may be calculated. The result for the sample shown is 72 MΩ/cm which is similar to that found in CPAN produced electrochemically.[38] A second film sample similar to that shown in Figure III-1 yielded 4.8 MΩ/cm. Though this does not speak well of the reproducibility, it does show that values can be obtained that are consistent with films produced by other methods. Though cracked and brittle, a value of 250 kΩ/cm was obtained for a heavily treated sample. No optical spectra was available due to the grainy character of the film. For comparison, Figure III-6 shows the plot for an untreated film. Resistance here is in the gigaohm range.

Figure III-7 shows the plot for the film shown in Figure III-4. Recall this film showed mixed patches of PAN and CPAN in an opaque film. The symmetric shift about the origin is very interesting and is something akin to diode behavior. From -15 to -3 V, the resistance is 572 kΩ/cm and is 621 kΩ/cm from +3 to +15 V. However, from -3 to +3 V, the value is 1.0 MΩ/cm, or almost twice that
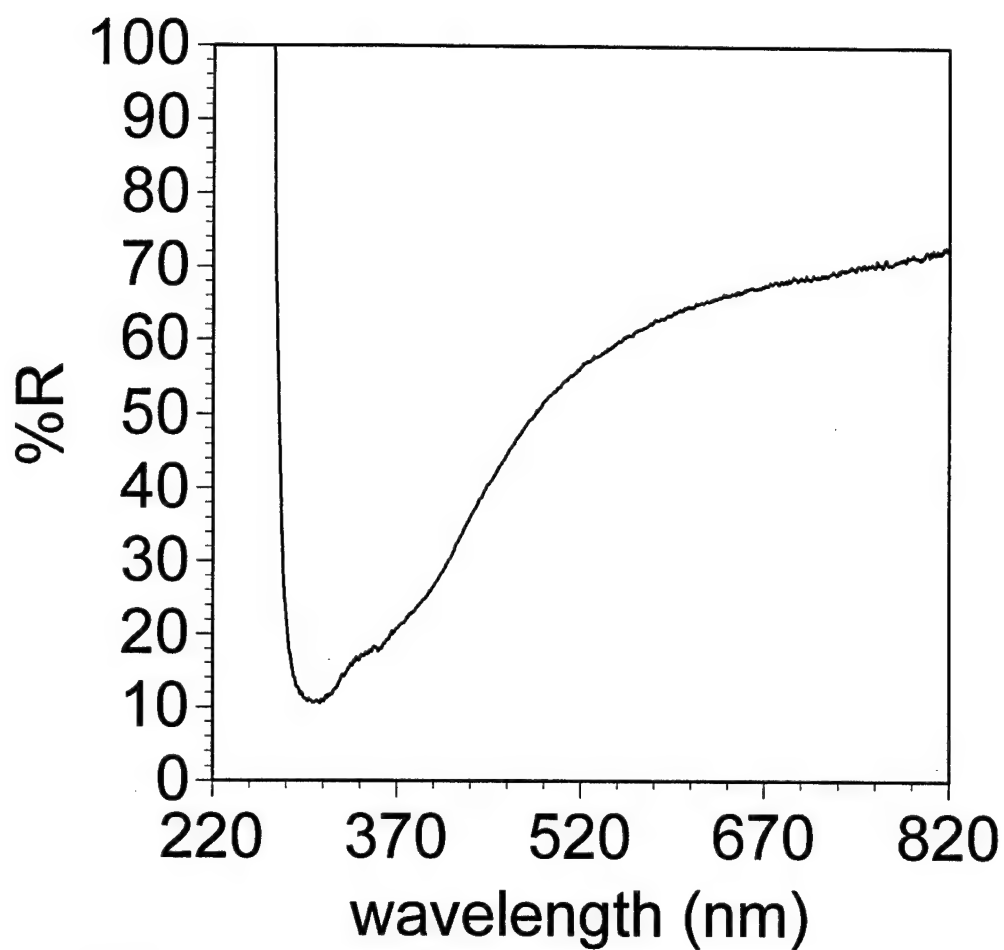
Figure III-4 Reflectance spectrum of a CPAN film derived from water washed fibers treated with 0.1M NaOCH₃/ethylene glycol solution at 60°C for 1 hour

outside this range. Since diodes are composed of junctions of p and n type semiconductors, it is possible that the junctions between PAN and CPAN domains are behaving in a similar fashion.

Attempts were made to reduce the resistance and gain consistency in the measured values by utilizing higher concentrations of PAN with base added directly, and raising the oven temperature from 60°C to 130°C. Both methods resulted in films that did not hold up very well. Higher concentration samples cracked upon cooling and those annealed at higher temperatures cracked upon contact sputtering. Though these results were discouraging, further work utilizing two solution mixing may yet yield satisfactory results.
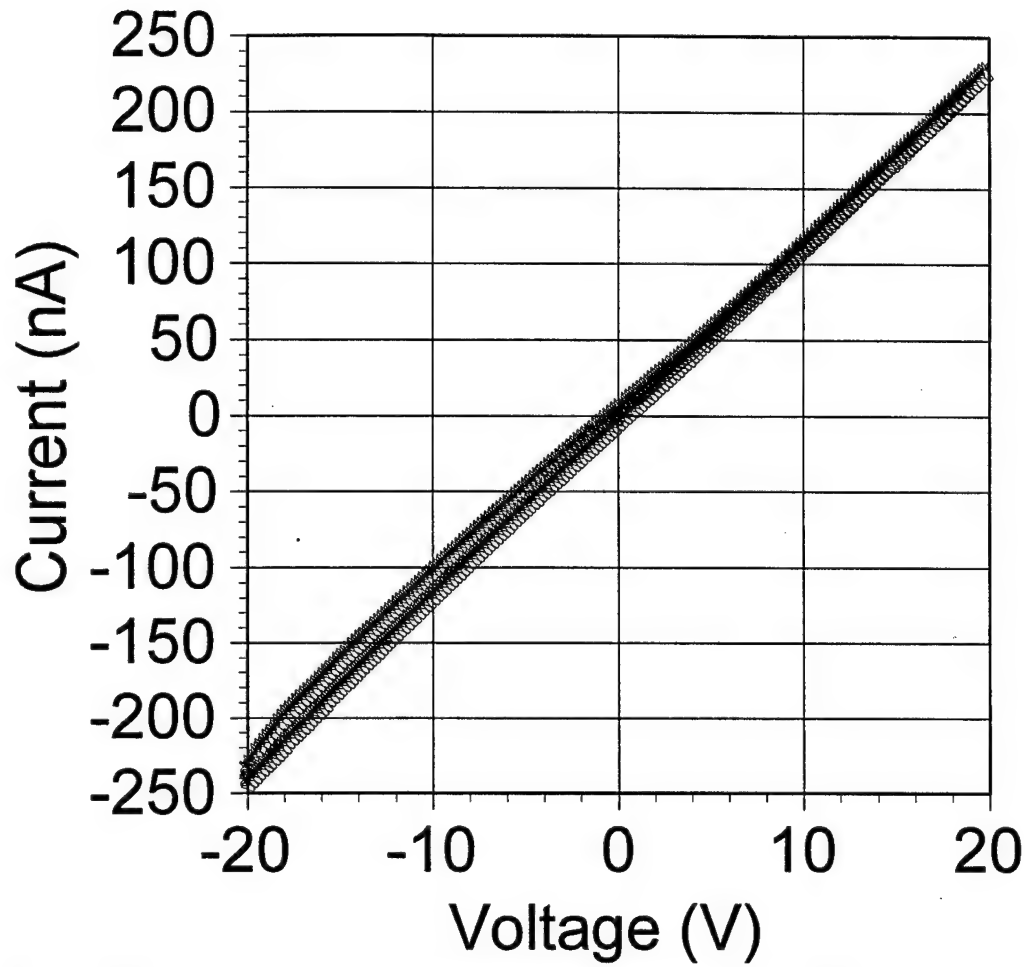
Figure III-5 Average two point resistance measurement of the film in Figure III-1.
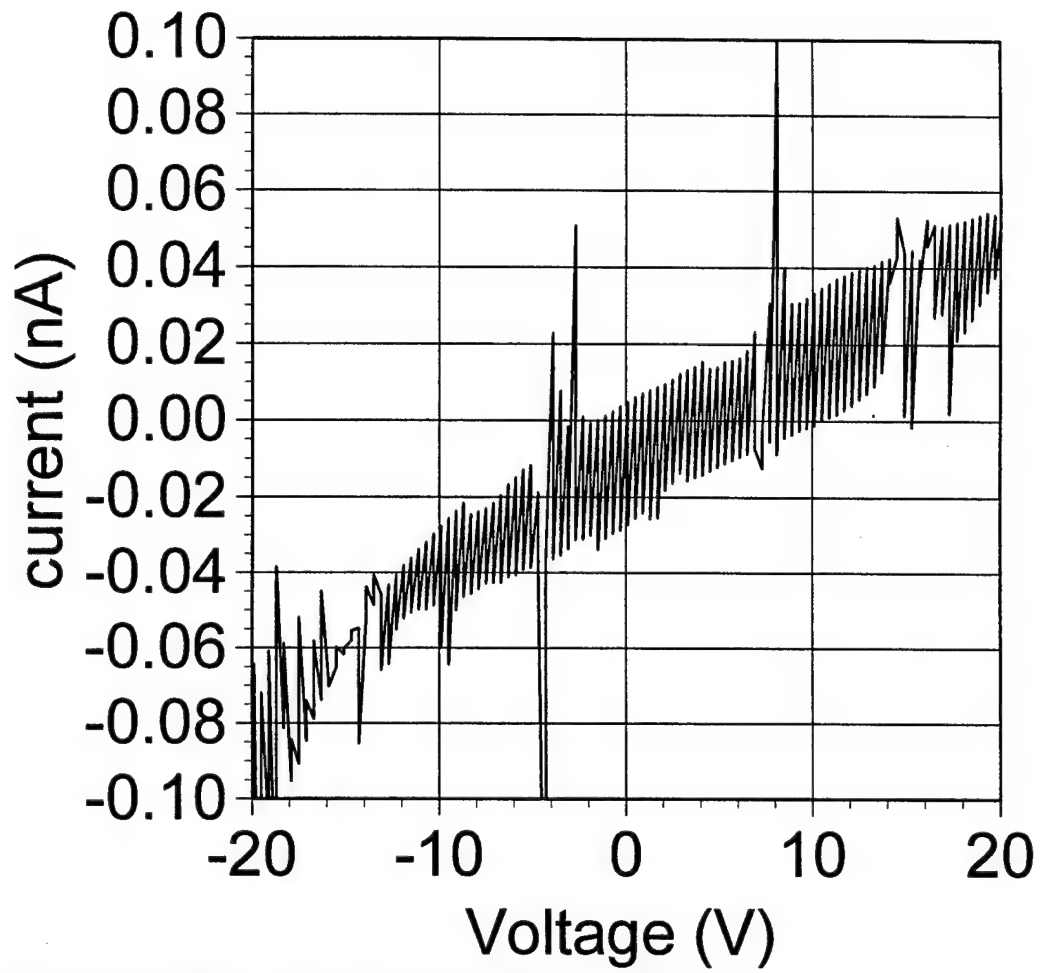
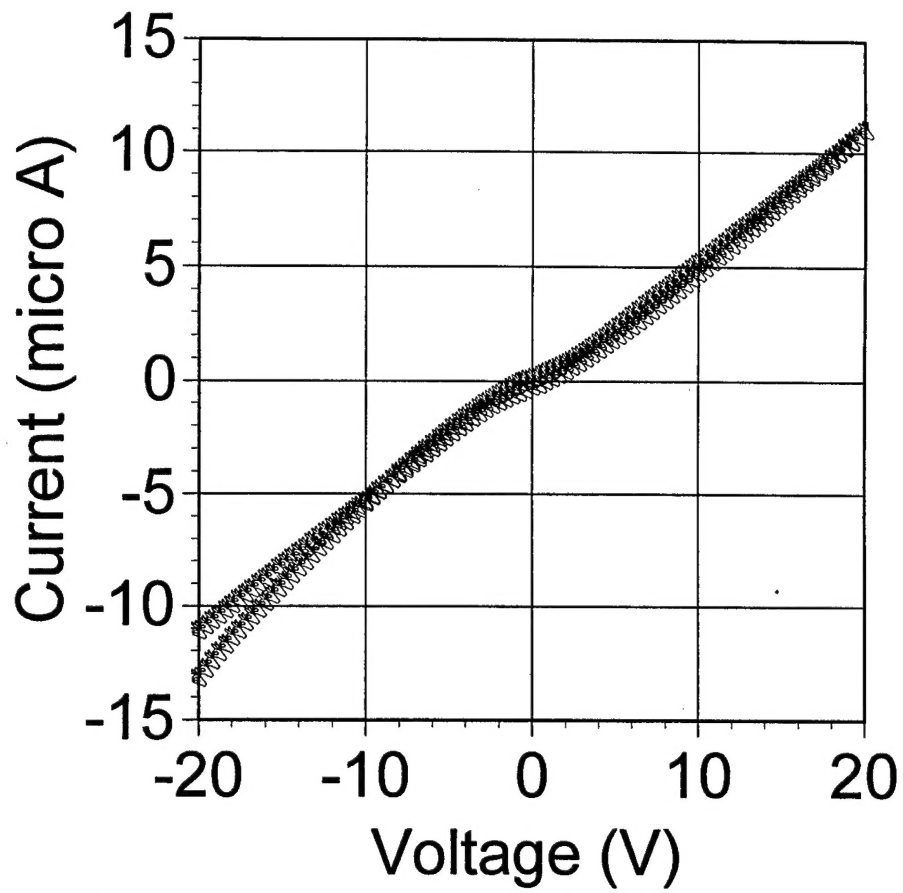Figure III-6 Average two point measurement of the film in Figure III-2.

Figure III-7 Average two point measurement of the film in Figure III-4.

CONCLUSION

Though not completely characterized, the results of the first chapter have shown that the photoreaction of R-11 with TiO_2 and a suitable hole scavenger proceeds via an efficient chain mechanism. The presence of an induction period, high photonic efficiency, and post irradiation effects all support this conclusion. Our inability to characterize the reaction with a simple rate law points to inhibition of the reaction at longer times, perhaps by catalyst poisoning. Further investigation is required to positively identify this mechanism.

Although not conclusive, it appears ground CPAN fibers can initiate photoreductions similar to those triggered by TiO_2. The reaction rates are much slower, but the possibility that photogenerated electrons are available for initiating chemical reactions is promising. Further investigation is warranted so that conditions may be found that would significantly increase the efficiency of this photoreaction.

CPAN films were made that showed optical and electrical data that is on par with results previously reported for films produced via other methods. This is interesting in that this method is much simpler and requires conditions milder than several other published techniques. While reproducibility problems have not been solved, further work utilizing two solution mixing may yet yield satisfactory results.

66

REFERENCES

[1] Fujishima, A.; Honda, K.; Nature, 1972, 37, 238.

[2] Ollis, D. F.; Al-Ekabi, H.; Eds. Photocatalytic Purification and Treatment of Water and Air; Elsevier: Amsterdam, 1993.

[3] a) Wu, C.-G.; DeGroot, D. C.; Marcy, H. O.; Schindler, J. L.; Kannewurf, C. R.; Bakas, T.; Papaefthynion, V.; Hirpo, W.; Yesinowski, J. P.; Liu, Y. -J.; Kanatzidis, M. G. J. Am. Chem. Soc. 1995, 117, 9229. b) Dalas, E.; Sakkopoulos, S.; Vitoratos, E.; Marolis, G.; Kobotiatis, L. J. Mat. Sci. 1993, 28, 5456. c) McElvain, J.; Heeger, A. J.; J. Appl. Phys. 1996, 80, 4755.

[4] Shen, T.-L.; Wooldridge, P. J.; and Molina, M. J.; In *Composition, Chemistry, and Climate of the Atmosphere*; Singh, H. B.; Ed.; Van Nostrand Reinhold: 1995; Chapter 12.

[5] Ravishankara, A. R.; Lovejoy, E. R. *J. Chem Soc., Faraday Trans*. **1994**, *90*, 2159.

[6] Kumaran, S. S., Su; M.-C., Michaail, J. V.; and Wagner, A. F.; *J. Phys. Chem.* **1996**, *100*, 7533-7540.

[7] Ogura, K., Kobayashi, W.; Migita, C. T. ; and Kaku, K.; *Environ. Tech.* **1992**, *13*, 81-88.

[8] Alfassi, Z. B.; Heusinger, H.; *Radiat.. Phys. Chem.* **1983**, *6*, 995-1000.

[9] a) Nielson, P. H.; Bjerg, P. L.; Nielson, P.; Smith, P.; Christensen, T. H.; *Environ. Sci. Tech.* **1996**, *30*, 31-37. b) Shorter, J. H.; Kolb, C. E.; Crill, P. M.; Kerwin, R. A.; Talbot, R. W.; Hines, M. E.; Harriss, R. C.; *Nature* **1994**, *377*, 717-719.

[10] Choi, W.; Hoffmann, M. R.; *Environ. Sci. Tech.* **1995**, *29*, 1646-1654.

[11] Stanbury, D. M.; Reduction Potentials Involving Inorganic Free Radicals in Aqueous Solution, [*Adv. Inorg. Chem.* **1989**, *33*, 69-138].

[12] Ward, M. D.; White, J. R.; Bard, A. J. *J. Am. Chem. Soc.* **1983**, *105*, 27-31.

[13] *CRC Handbook of Chemistry and Physics*; 73RD ed.; CRC Press: Cleveland, 1992.

[14] Linsebigler, A. L.; Guangquan, L.; Yates, J. T. Jr.; *Chem. Rev.* **1995**, *95*, 735-758.

[15] Sabin, F.; Turk, T.; Vogler, A. *J. Photochem. Photobiol. A: Chem.* **1992**, *63*, 99.

[16] Weaver, S.; Mills, G. *J. Phys. Chem. B*, **1997**, *101*, 3769.

[17] Hinshelwood, C. N.; in *Kinetics of Chemical Change*, Oxford University Press, London, 1942, p. 161.

[18] Caldin, E. F.; In *Fast Reactions in Solution*; John Wiley & Sons Inc., New York, London; 1964, p.122.

[19] Gratzel, M.; Kalyanasundaram, K.; Eds. *In Kinetics and Catalysis in Microheterogeneous Systems*; Marcel Dekker, Inc., New York; 1991, p. 311.

[20] Horvath, A. L.; In *Halogenated Hydrocarbons: Solubility-Miscibility with Water*, Marcel Dekker, Inc., New York; 1982, p. 661.

[21] a) Hatchard, C. G.; Parker, C. A. *Proc. Roy. Soc. A* **1956**, *235,* 518. b) Heller, H. G.; Langan, J. R. *J. Chem. Soc., Perkin Trans. II* **1981**, 341.

[22] Augustynski, J. In *Structure and Bonding. Solid Materials*; Springer-Verlag: Berlin, 1988; Vol. 69, p. 51.

[23] Choi, W.; Hoffman, M. R. *J. Phys. Chem.* **1996**, *100*, 2161-2169.

[24] Colombo, R.; Bowman, ? *J. Phys. Chem.* **1996**, *100*, 18445.

[25] Sahyun, M. R. V.; Serpone, W. *Langmuir* **1997**, *13*, 5082.

[26] Hoffmann, M. R.; Martin, S. T.; Choi, W.; Bahnemann, D. W. *Chem. Rev.* **1995**, *95*, 69-96

[27] Weaver, S. Ph.D. Thesis, Auburn University, **1998**, p.44.

[28] Neta, P.; Huie, R. E.; Ross, A. B. *J. Phys. Chem. Ref. Data* **1988**, *17*, 1027.

[29] a) Huang, Z. -Y.; Barber, T.; Mills, G.; Morris, M. -B. *J. Phys Chem.* **1994**, *98*, 12746. b) Hoffman, A. J.; Yee, H.; Mills, G.; Yee, H.; Hoffmann, M. R. *J. Phys. Chem.* **1992**, *96*, 5546.

[30] Friedlander, H. N. Peebles, L. H. Jr.; Brandrup, J.; Kirby, J. R.; *Macromolecules* **1968**, *1*, 79-86.

[31] Chung, T. -C.; Schlesinger, Y.; Etemad, S.; Macdiarmid, A. G.; Heeger, A. J.; *J. Poly Sci.* **1984**, *22*, 1239-1246.

[32] Farges, J.-P., Ed.; In *Organic Conductors: Fundamentals and Applications*;, Marcel Dekker, Inc., New York; 1994, p. 539.

[33] Patil, A. O.; Heeger, A. J.; Wudl, F.; *Chem. Rev* **1988**, *88*, 183-200.

[34] Used with permission from Kurt Winkelmann.

[35] Ulman, Abraham, Ed.; In *Characterization of Organic Thin Films*;; Butterworth-Heinemann, Stoneham, MA, USA; 1995, Chs 1 and 2.

[36] Chung, T.C.; Schlesinger, Y.; Etemead, S.; MacDairmid, A. G.; Heeger, A. J. *J. Poly. Sci: Poly. Phys. Ed.* **1984**, *22*, 1239.

[37] Ohring, M.; In *The Materials Science of Thin Films*; p. 473, Academic Press, San Diego, 1992.

[38] Reicha, F. M. *Poly. Intl.* **1996**, *41*, 463.